



Published in final edited form as:

*Environ Sci Technol.* 2018 May 01; 52(9): 5027–5047. doi:10.1021/acs.est.7b06487.

## Insight into Multiple and Multilevel Structures of Biochars and Their Potential Environmental Applications: A Critical Review

Xin Xiao<sup>†,‡</sup>, Baoliang Chen<sup>\*†,‡</sup>, Zaiming Chen<sup>§</sup>, Lizhong Zhu<sup>†,‡</sup>, and Jerald L. Schnoor<sup>||</sup>

<sup>†</sup>Department of Environmental Science, Zhejiang University, Hangzhou 310058, China

<sup>‡</sup>Zhejiang Provincial Key Laboratory of Organic Pollution Process and Control, Hangzhou 310058, China

<sup>§</sup>Department of Environmental Engineering, Ningbo University, Ningbo 315211, China

<sup>||</sup>Department of Civil and Environmental Engineering, University of Iowa, Iowa City, Iowa 52242, United States

### Abstract

Biochar is the carbon-rich product of the pyrolysis of biomass under oxygen-limited conditions, and it has received increasing attention due to its multiple functions in the fields of climate change mitigation, sustainable agriculture, environmental control, and novel materials. To design a “smart” biochar for environmentally sustainable applications, one must understand recent advances in biochar molecular structures and explore potential applications to generalize upon structure–application relationships. In this review, multiple and multilevel structures of biochars are interpreted based on their elemental compositions, phase components, surface properties, and molecular structures. Applications such as carbon fixators, fertilizers, sorbents, and carbon-based materials are highlighted based on the biochar multilevel structures as well as their structure–application relationships. Further studies are suggested for more detailed biochar structural analysis and separation and for the combination of macroscopic and microscopic information to develop a higher-level biochar structural design for selective applications.

## 1. INTRODUCTION

Biochar is a solid, carbon-rich product obtained from the thermal treatment of biomass pyrolyzed under an oxygen-limited atmosphere.<sup>1</sup> The massive production of agricultural waste in the world provides an abundant source for biochar preparation. It was estimated that both China and the USA have ~1.4 billion tons of annual agricultural biomass waste production, which has the potential to produce ~420 Mton biochar per year.<sup>2,3</sup> Other countries, such as Zimbabwe<sup>4</sup> and Ghana,<sup>5</sup> can produce 3.5 and 7.2 Mton of biochar annually, respectively. Increasing attention is being devoted to biochar applications in the fields of agriculture, climate change, environmental remediation, and materials science.

\*Corresponding Author: B. Chen. Phone: 0086-571-88982587; fax: 0086-571-88982587; blchen@zju.edu.cn.

The authors declare no competing financial interest.

Supporting Information

The Supporting Information is available free of charge on the ACS Publications website at DOI: [10.1021/acs.est.7b06487](https://doi.org/10.1021/acs.est.7b06487).

Biochar, originating 2000 years ago in the Amazon Basin as *terra preta* black soil, is a long-lasting additive producing rich agricultural soil.<sup>6,7</sup> In 2006, Johannes Lehmann commented that biochar could lock-up carbon from the atmosphere in the soil to mitigate climate change.<sup>8,9</sup> Later on, the sorption behaviors of biochar toward different organic pollutants and heavy metals were investigated for environmental remediation in 2008<sup>10</sup> and 2009,<sup>11</sup> respectively. Recently, biochars were developed into functional materials due to their cheap and sustainable properties.<sup>12</sup> The diverse functionalities of biochar suggest multipurpose applications, but they require deeper understanding for smart biochar design.

Many different biomass materials can be utilized to produce biochars for different purposes. The challenge is how to choose the right precursors and preparation procedures to obtain biochars for specific purposes. The preparation methods for biochars could be classified as pyrolysis, gasification, hydrothermal carbonization, and flash carbonization.<sup>13</sup> Compared to biomass, which is a living, colorful, and water-rich material with a low surface area, biochar is a black carbon-rich product with a high surface area and no cellular structure. The transformation of biomass during pyrolysis alters the structure in different ways and further influences the properties of biochar. Typical properties vary with the pyrolysis temperature and are listed in Figure 1. With increasing pyrolysis temperatures (100–700 °C), the biomass color changes from its original color to black, and the product yield (typically 91%–14% for pine needle-derived biochars<sup>10</sup>), polarity, hydrogen content (H%) (typically 6.2–1.3% for pine needle-derived biochars<sup>10</sup>), oxygen content (O%) (typically 42–11% for pine needle-derived biochars<sup>10</sup>), and albedo of the biochars decreased. In contrast, the carbon content (C%) (typically 50%–86% for pine needle-derived biochars<sup>10</sup>), ash percentage (typically 13%–49% for rice straw-derived biochars<sup>14</sup>), aromaticity, pH, surface area (typically 0.65–490 m<sup>2</sup> g<sup>-1</sup> for pine needle-derived biochars<sup>10</sup>), and zeta potential ( $\zeta$ ) increased with increasing pyrolysis temperature (100–700 °C). The hydrophobicity of biochar increases and then decreases with pyrolysis temperature, as recent studies show that aromatic surfaces are intrinsically mildly hydrophilic, but adsorbed hydrocarbon contaminants provide the hydrophobicity of the aromatic surfaces in the midtemperature range.<sup>15</sup> The diversity of biochar with regards to its properties, structures, applications, and mechanisms inevitably requires a clarification of the relationships among variables, especially for structure-application relationships, which are indispensable and of fundamental concern.

Several reviews summarized the applications of biochar.<sup>16,17</sup> For example, researchers reviewed the sorption properties of biochars toward both organic and inorganic contaminants.<sup>18,19</sup> Applications for climate<sup>13</sup> and agriculture<sup>20</sup> were also reviewed. In 2015, Liu et al. suggested that biochars be considered as functional carbon platform materials considering their low-cost and sustainability, thus increasing the applications of biochar into the field of novel materials.<sup>12</sup> These reviews made great strides to summarize and characterize biochar applications, which will greatly promote research. However, the body of literature regarding the structure of biochar, especially with regards to biochar applications, is inadequate. Despite considerable research and reviews on biochar, a critical review on the structure and application relationships of biochar is urgently needed to understand and develop these novel materials.

A large number of precursor biomass and different preparation methods offers selective utilization opportunities for biochar, despite the enormous uncertainty and heterogeneity of biochar structures. To investigate the aromatic structure of biochar, many researchers suggested graphene and/or graphite as an ideal model.<sup>1,21,22</sup> Nonetheless, the biomass will go through aromatization and graphitization processes at high pyrolysis temperatures ( > 500 °C), but the heterogeneous nature and structures of middle pyrolysis temperature-derived biochar are not fully comprehended. Additionally, besides the major element “carbon”, many other elements exist in biochar, which affects the corresponding role, function, and application of the material. The elements form different phases within biochar, which provides unique physical properties. The surface chemistry of biochar becomes critical because the interfaces between biochar and the aqueous phase provides important sites for sorption and reaction, including surface functional groups, surface radicals and surface charge. Heterogeneous biochar can be viewed as an aggregation of multiple molecules, containing both skeletal and small extracted molecules (Figure 2). To date, a few studies have focused on biochar structures, but a systematic summary detailing the structures of biochars is still lacking. In 2017, a quaternary structural model of biochars was proposed from the macroscopic to microscopic level for high pyrolysis temperature-derived biochars.<sup>21</sup> In this review, we will interpret the multiple and multilevel structures of biochars from their elements, to phases, to surfaces, and to molecular structures (Figure 2). With the knowledge of biochar structures, their relationships to applications are further discussed in four different areas: agriculture, fertilizers; climate, carbon sequestration; environment, sorbents; and materials, functionalization. We summarize the advances in biochar structures and applications and begin to establish structure–application relationships with the overall goal to design smart biochars for environmentally sustainable applications.

## 2. MULTIPLE AND MULTILEVEL STRUCTURES OF BIOCHARS

### 2.1. Elements.

The elements present are the fundamental building blocks of biochars. During the pyrolysis of biomass, elements within the biochar experience different physicochemical processes and form different species and products, thus contributing to the diversity of biochars. The species and functions of these elements are listed in Table 1. These elements are part of global geochemical processing, and they have different mass percentages and functions within biochars. Among these elements, C, H, O, and N are the most common elements and generally contribute to the major structures of biochar; Si, Fe, P, and S show a wide range of mass percentages in specific biochars, whereas some elements (such as Si, N, P, S, and Fe) are nutrient elements for specific plants. In global geochemistry cycles, some elements (C, H, O, S, and N) are bidirectional in their cycling from the atmosphere to the earth, whereas other elements (P, and Si) are unidirectional due to the lack of atmospheric species. The multiple roles of multiple elements endow biochar with unique structures and functions. Thus, in this section, the chemical state, species, functions, applications, and geochemistry cycling involved with biochars are discussed.

**Carbon.**—Carbon is the most important and the most abundant element in biochars. The carbon species within biochars can be classified as carbonate and bicarbonate in the

inorganic phase and aliphatic carbon, aromatic carbon and functionalized carbon in the organic phase (Table 1). It is quite difficult to precisely differentiate these carbon species. During the pyrolysis process, the inorganic carbon may transform from hydrated carbonate to bicarbonate, carbonate or even be lost in the form of CO<sub>2</sub>, depending on the type of inorganic crystal.<sup>38</sup> As for the organic carbon, the carbon transformed from cellulose/hemicellulose/lignin in the biomass becomes aliphatic carbon in the middle pyrolysis temperature-derived biochars, and further also results in aromatic carbon at high pyrolysis temperatures after dewatering, cracking, and aromatization reactions.<sup>39</sup> These transitions were confirmed by Fourier transform infrared spectroscopy (FT-IR),<sup>10,40</sup> Raman spectroscopy,<sup>41</sup> cross-polarization magic angle spinning (CPMAS), solid <sup>13</sup>C nuclear magnetic resonance spectroscopy (NMR),<sup>42</sup> and other characterizations. More recently developed technologies were applied to gather more chemical information about the carbon species in biochar, such as two-dimensional <sup>13</sup>C NMR.<sup>43,44</sup> These characterization methods can distinguish between atomic and alkyl carbons; however, it is still difficult to differentiate the functionalization of the carbon. The chemical species of carbon is critical for applications in agriculture, ecosystems, and carbon sequestration because the chemical species determine the stability and reactivity of the carbon in biochar.

**Silicon.**—Although not all of the biomass or agricultural waste that is pyrolyzed into biochars contains silicon, silicon-rich biomass such as rice straw, rice husk, and corn straw are vital feedstocks for biochar production and essential plants for food production.<sup>14,45</sup> In fact, silicon is a required nutrient for silicophilic plants (such as rice, maize, wheat, and barley),<sup>46</sup> protecting these plants from insects, heavy metals, infestation, light, and drought.<sup>47–49</sup> Moreover, our previous studies found that the silicon in biochars contributed to the sorption and retention of heavy metals (such as aluminum<sup>26,50</sup> and cadmium<sup>24</sup>) in aqueous systems. The dissolution of silicon from biochars to form monosilicic acid in water<sup>25</sup> was found to be important in the biochar sorption of metals.

Our research group first investigated silicon transformation in rice straw derived biochars under different pyrolysis temperatures.<sup>14</sup> In the biomass, silicon existed as phytoliths in the form of silicic acid and polymeric silicon that can easily dissolve.<sup>45</sup> During charring, the silicon becomes dehydrated and polymerized, and upon further pyrolysis, and the polymeric silicon was partially crystallized. Rice straw biochars pyrolyzed at high temperature display higher silicon dissolution than low pyrolysis temperature-derived biochars. Additionally, Si-rich biochars show much higher silicon dissolution tendencies than their corresponding ash or soil, which contain large amounts of silicon in the form of silicate.<sup>14,51</sup> Because many arable lands in the world are suffering from silicon depletion, the Si-rich biochars with high silicon dissolution capacities may provide a slow-release Si-fertilizer for soil.

Silicon represents a major fraction of the inorganic phase in Si-rich biochars (composing ~38% of the mass in rice straw ash),<sup>14</sup> and it seems to be separated from the organic matter in biochars. However, according to the results of scanning electron microscopy-energy dispersive spectroscopy (SEM-EDS), a mutual protection exists between carbon and silicon under different pyrolysis temperatures. The carbon layer protects the silicon from dissolution under low pyrolysis temperatures, and the silicon layer protects the carbon from loss under

high pyrolysis temperatures.<sup>14</sup> Our study further indicated that the silicon may promote recalcitrance and stability in biochars.<sup>52</sup>

Figure 3 provides a schematic of the coupling cycles of carbon and silicon in biochar and the terrestrial ecosystem. In the environment, the Si-rich biomass takes-up CO<sub>2</sub> from the atmosphere and silicic acid from the soil solution. However, with increased charring temperature, the interlaced C–Si content starts to separate and form corresponding crystals, which are stable over long periods. With burning and dissolution over a long period of time, the carbon and silicate minerals release CO<sub>2</sub> and silicic acid which becomes available to plants, thus completing the geochemical cycle. This type of C–Si coupling illustrates the vital role that biochars play in the geochemical cycling of these essential nutrient elements. It also indicates the need for more research for a better understanding of the role of biochar in global carbon and silicon balances as well as the important agricultural function of silicon in biochar.

**Hydrogen.**—There are three species of hydrogen that exist in biochars: aliphatic hydrogen, aromatic hydrogen, and active functionalized hydrogen (Table 1). For typical biochar, the hydrogen weight percentage in organic matter decreases from ~6% at low pyrolysis temperatures to ~1% at high pyrolysis temperatures.<sup>10</sup> The low hydrogen content makes it more difficult to characterize biochars by FT-IR or H NMR. Therefore, the speciation of hydrogen within biochar is qualitatively assessed by elemental analysis and characterizing other elements, such as carbon or oxygen. Because the H/C atomic ratio for aliphatic organic matter in biochars is approximately 2.0, and the H/C atomic ratio of aromatic organic matter decreases with larger fused aromatic clusters, the H/C atomic ratio is widely regarded as an aromaticity index for biochars.<sup>22</sup> Compared to the stable aliphatic and aromatic hydrogen in biochars, more uncertainty exists regarding the active functionalized hydrogen. Active hydrogen atoms in functional groups can be associated/dissociated under proper pH conditions, and this is easily probed by a pH meter. The association/dissociation interaction may lead to formation of intra- and intermolecular H-bonds, causing different polarities between the bulk biochar and its surface.<sup>53</sup> Hydrogen bonds (D–H···A) are generated between the biochar surface and ionizable molecules by sharing protons.<sup>54</sup> Therefore, hydrogen acts as an important building block for biochar structures, and it plays a key bridging role in biochar sorption toward ionizable molecules.

**Oxygen.**—In the inorganic phase of biochars, oxygen mainly exists in the form of metallic oxides, hydroxides, or inorganic clusters such as carbonate, bicarbonate, and sulfate (Table 1). Inorganic oxygen is generally stable and contributes to the alkalinity of biochars. In the organic phase of biochars, oxygen atoms are mostly attached to carbon atoms, forming different types of functional groups, including hydroxyl, epoxy, carboxyl, acyl, carbonyl, ether, ester, and sulfonic groups (Table 1). Because the oxidation process in natural environments regularly induces oxygen into the organic structures of biochars, the O/C atomic ratio is thus widely considered to be an indicator of the degree of aging/oxidation undergone by biochars.<sup>55–58</sup> This oxidation induces the formation of carboxyl groups, and it could somehow benefit the sorption of aluminum<sup>59</sup> and lead.<sup>60</sup> The release of CO<sub>2</sub> from carboxyl groups may be an important reaction in the labile fraction of biochars, although the

structural framework to which the carboxyl groups were attached might be considered to be stable carbon. More details are discussed in the section on surface functional groups because oxygen-containing groups contribute significantly to biochar functional groups.

**Nitrogen.**—In biomass, nitrogen mainly contributes to the peptide bond in protein. Normally, biochar feedstocks such as plants and wood are nitrogen-poor materials due to their rather low protein content, whereas materials such as grass or leaves contain relatively higher protein contents and are nitrogen-rich materials. For example, casein, grass, and wood-derived biochars were reported as containing ~15%, ~7%, and 0.3–1 wt % nitrogen, respectively.<sup>10,61</sup> Although many researchers have studied nitrogen-rich biochars, only a few focused on the nitrogen speciation within biochars. Theoretically, the structures related to nitrogen contain pyrrole, pyridine, amine, imine, acylamide, nitroso, and nitro groups (Table 1). Reports indicate that the total nitrogen content within biochars increases and then slightly decreases with increasing pyrolysis temperature.<sup>10,61,62</sup> Knicker et al. identified a model biochar and suggested that the N forms are mainly pyrrole-N, amide-N, and pyridine-N.<sup>63</sup> During pyrolysis, peptide-N bonds were transformed to N-heteroaromatic carbon compounds, whereas some amide-N within biochars decreased with increasing pyrolysis temperature.<sup>61</sup> Pietrzak et al.<sup>64,65</sup> studied the reaction of ammonia/urea with coal and found that the nitrogen was introduced at 500–700 °C in the form of pyridinic-N and pyrrolic-N as well as imine-N, amine-N, and amide-N. For the pyridinic-N and pyrrolic-N, many studies on carbon materials (such as graphene<sup>66</sup>) were conducted with nitrogen-doped carbon materials to modify the electronic band structures, and they acted as the active sites for reaction. This may explain the observations that nitrogen-rich biochars show greater heat resistance but less chemical-oxidation stability than nitrogen-poor biochars.<sup>61</sup> After application into soil, the fate of extractable N becomes of research interest. By applying different extraction methods, different species of extractable N, including that from ammonia, amino sugars, amino acids, and total hydrolyzable forms, were found to decrease with pyrolysis temperature.<sup>67</sup>

In fact, there is uncertainty whether the extracted N comes from organic matter or inorganic matter in biochar. Nitro- and nitrito-N were also found in biochars derived from agricultural biomass (rice husk), forestry waste (sawdust), and wetland plants (*Acorus calamus*) at 650 °C.<sup>68</sup> However, the nitrogen content of biochars is usually too low to be considered a nitrogen fertilizer alone. The biochars with high C/N ratios have limited N availability, and additional nitrogen fertilizer might be needed to improve microbial and plant growth in soils.<sup>69–71</sup> For example, it was reported that 5% biochar combined with mineral fertilizer (containing 0.0134% N) shows remarkably higher promotion of oat growth than biochar alone.<sup>72</sup>

The nitrogen dynamics of biochars applied as additives in soil systems are of considerable interest, including the effects on nitrogen-sorption, nitrogen-fixation, nitrification, and N<sub>2</sub>O greenhouse gas (GHG) emissions. Multiple studies indicate that biochars show a high affinity for the sorption of ammonium nitrogen (NH<sub>4</sub><sup>+</sup>) by cation-exchange, but no influence on the removal of nitrate-N.<sup>73–77</sup> Ammonia sorbed onto biochars is reported to be bioavailable,<sup>78</sup> and thus biochars are regarded as a nutrient-retention additive to maintain the nitrogen in soil.<sup>73,79</sup> It is a soil “conditioner,” which improves the tilth, water holding

capacity, and nutrient holding capacity of soil.<sup>1</sup> Additionally, it stabilizes the carbon and nitrogen, thus reducing the emissions of GHGs (CO<sub>2</sub> and N<sub>2</sub>O). Biochars were reported to increase the biological nitrogen fixation proportion of common beans from 50% without biochar to 72% with 90 g kg<sup>-1</sup> biochar added,<sup>28</sup> and stimulated both the nitrification and denitrification processes with a result of reducing N<sub>2</sub>O emissions.<sup>80</sup> The reduction order of N<sub>2</sub>O emissions by giant reed-derived biochars additives in soils differed with pyrolysis temperatures, following the order BC200 ≈ BC600 > BC500 ≈ BC300 ≈ BC350 > BC400 (BC refers to biochar, the suffix number represents the preparation pyrolysis temperature of biochar).<sup>81</sup> The “electron shuttle” of biochar may facilitate the transfer of electrons to denitrifying microorganisms as well as the “liming effect” of biochars, which promote the reduction of N<sub>2</sub>O to N<sub>2</sub>, leading to a 10–90% decrease in N<sub>2</sub>O emissions in 14 different agricultural soils.<sup>82</sup> The carbon and nitrogen cycles are affected in three ways by biochar. (1) During biochar processing, carbon becomes more recalcitrant and nitrogen becomes less available, thus stabilizing the biochar product.<sup>83</sup> (2) Microbial and plant growth in soils with biochar additives are limited by the low nitrogen content, and less microbial growth stabilizes and reduces carbon mineralization.<sup>84</sup> (3) The sorption of NH<sub>4</sub><sup>+</sup> onto the carbon components of biochars improves the nitrogen retention in soil systems.

**Phosphorus.**—Unlike carbon, hydrogen, oxygen, and nitrogen, which are lost during the pyrolysis process, phosphorus does not volatilize at temperatures below 700 °C,<sup>16</sup> leading to an enhancement of phosphorus under typical pyrolysis temperatures. Ngo et al.<sup>85</sup> reported an overwhelming dominance of inorganic phosphorus compared to organic phosphorus in bamboo-derived biochar produced at 500–600 °C. Considering the fact that the phosphorus in biomass is mostly organic (such as monophosphate and phosphate diesters<sup>62</sup>) (Table 1), the phosphorus species transformation during pyrolysis is dramatic and discussed by Uchimiya and Hiradate.<sup>86</sup> Using <sup>31</sup>P NMR analysis, they proposed that the phytate is converted to inorganic phosphorus from manure and plant-derived biochars at 350 °C.<sup>86</sup> Regarding inorganic phosphorus, the pyrophosphate (P<sub>2</sub>O<sub>7</sub><sup>4-</sup>) in plant material was persistent in biochars pyrolyzed at temperatures up to 650 °C and the orthophosphate (PO<sub>4</sub><sup>3-</sup>) became the sole P-species for manure biochars at pyrolysis temperatures higher than 500 °C.<sup>86</sup>

Similar to silicon, phosphorus is an important nutrient for plant and microbe growth. The geochemical cycle of phosphorus is also unidirectional from land to sea because there is no gaseous phosphorus species, and it is difficult to transport ocean phosphorus back to the land ecosystem except via the slow crustal plate movement of subduction. Thus, making a slow releasing P-additive in the form of biochar was proposed to retain more phosphorus in soil.<sup>87</sup> The effects of the pH and other anions and cations on the release of phosphorus were further investigated.<sup>88</sup> These results report that high pH soils greatly hinder the release of phosphorus.<sup>88</sup> However, other anions could enhance the orthophosphate (PO<sub>4</sub><sup>3-</sup>) release due to competing ion exchange reactions.<sup>89</sup> Competing cations will decrease the release of P due to the formation of precipitates.<sup>89</sup> Furthermore, phosphate in biochars could immobilize some heavy metals by precipitation, such as β-Pb<sub>9</sub>(PO<sub>4</sub>)<sub>6</sub> precipitates<sup>11</sup> or insoluble hydroxypyromorphite Pb<sub>5</sub>(PO<sub>4</sub>)<sub>3</sub>(OH).<sup>90</sup> In summary, phosphorus in biomass was

transformed from organic P to inorganic P via carbonization and can then serve as a nutrient for the soil system or as a sorption site for heavy metals.

**Other Elements.**—In addition to the major elements mentioned above, there are other trace elements that could exist in biochar. Under most circumstances, these elements constitute only a small fraction of biochars (typically with the concentration level of mg kg<sup>-1</sup><sup>28</sup>). Dopants may also be added to provide special chemical properties to biochars. Nutrient elements such as Na, K, Ca, Mg, and Mn<sup>88,91–96</sup> constitute important fractions of biochars, and other elements designed to functionalize biochars may be added. For example, ~20% Mg (in the form of MgO) was loaded onto biochars and increased CO<sub>2</sub> capture from ~0.1 to ~5 mol CO<sub>2</sub> per kg biochar.<sup>35</sup> By inducing sulfuric acid groups onto biochars, a solid acid catalyst can be formed for transesterification,<sup>97,98</sup> hydrolysis reactions,<sup>30,99</sup> and biodiesel production.<sup>100,101</sup> Sulfonation is known to increase the solubility of carbon materials in aqueous systems.<sup>29</sup> Early in 2011, our research group<sup>31</sup> reported on novel magnetic biochars prepared by the coprecipitation of Fe<sup>3+</sup>/Fe<sup>2+</sup> onto orange peels followed by pyrolysis. These magnetic biochars (with ~13 wt % Fe) show efficient sorption performance toward organic pollutants and almost thrice the sorption capacity toward phosphate compared to nonmagnetic biochars pyrolyzed at 700 °C. Magnetic biochars can be easily separated from wastewater and thus have great potential for environmental and agricultural applications. Manganese oxide-modified biochars have been reported to benefit the sorption of arsenate, lead, and copper.<sup>102,103</sup> Moreover, some elements have a great impact on shaping the biochar structure, such as Zn as a pore-maker and Fe for its promotion of graphitization.<sup>32</sup> In addition, some trace metals (such as Cu and Al) show promise for producing favorable structural properties in biochars, but they must be evaluated for their toxicity prior to being adopted as soil additives.<sup>104,105</sup> There are many other elements that could be bonded to biochars, but we must first understand their toxicity, speciation within biochars during pyrolysis, and influence on biochar carbon stability and structure.

## 2.2. The Phases.

**Organic Phase.**—The bulk of biochar was formed via forming massive chemical bonds between the mentioned elements. Previous researchers, without knowing the exact structure, considered biochar to be a solid phase. Furthermore, this solid biochar could be subdivided into various different phases. Our knowledge of biochar phases continues to evolve over time (Figure 4). Besides classifying biochars into organic and inorganic phases, we may also consider their aliphatic and aromatic chemical nature.<sup>106–108</sup> In terms of their sorption mechanisms, we can differentiate biochar into an organic-partitioning and a surface adsorption phase, which comprises the total sorption of organic molecules.<sup>10,109–111</sup> Furthermore, on the basis of solubility, biochar can be classified into a dissolved phase and an undissolved phase;<sup>25,112–114</sup> and in view of carbon stability, a labile phase can be defined in which the carbon fraction can be mineralized under natural soil conditions, while the stable phase remains recalcitrant.<sup>115–118</sup> With increasing pyrolysis temperature, biochar undergoes dehydration, disruption of the organic components, and successive aromatization. The aliphatic labile portion and dissolved-phase fraction decrease, whereas the aromatic stable portion and undissolved-phase increase. It was reported that the labile carbon percentage of sugar cane-derived biochars decreased from 1.08% at a 350 °C pyrolysis



temperature to 0.29% at a 550 °C pyrolysis temperature.<sup>118</sup> Additionally, the dissolved carbon percentage decreased from ~14% in 100 °C-derived dairy manure biochar to ~0.2% in 700 °C-derived dairy manure biochar at a pH of ~12.<sup>25</sup>

Recently, four different chemical phases and physical states were proposed: (1) a transition phase with the preserved crystalline character of the precursors; (2) an amorphous phase with cracked molecules and aromatic polycondensations; (3) a composite phase with poorly ordered graphene stacks; and (4) a turbostratic phase with disordered graphitic crystallites.<sup>40</sup> The aliphatic phase, labile phase, partition phase, and dissolved phase are similar but not the same as each other. The aromatic phase, stable phase, adsorption phase, and undissolved phase are also similar but not the same as each other. For example, unlike the other phases where the pH has little effect, the dissolved carbon phase is strongly affected by the pH.<sup>25</sup> Part of the dissolved carbon phase can be oxidized to CO<sub>2</sub>, indicating that the dissolved phase partially contributes to the labile phase.<sup>113</sup> The labile carbon fraction is related but not the same as the dissolved carbon fraction.<sup>117</sup> A portion of the biochar aromatic phase represents the labile form in biochars but may not be persistent.<sup>108</sup> Even though there are various definitions and research on the organic phase of biochar, more investigations are needed, especially regarding the separation methods, structure–function relationships, biological effects, and environmental fate of these different phases including their nanoformed particles.

**Inorganic Phase.**—Because of the existence of minerals in biomass, biochars are actually a mixture of interlaced inorganic–organic structures. These inorganic phases interact with and influence the organic phases in biochars and thus impact their properties, making the understanding of mineral phase transformations during pyrolysis of great importance.

Figure 5 summarizes the possible phase transformations of several typical mineral components generated during biomass pyrolysis. Possible reactions that could occur in the inorganic phase during pyrolysis include dehydration, dechlorination, polymerization, decarboxylation, crystallization, and reduction. For example, the silicic acid within the rice straw will polymerize to form polymer silicon and further crystallize to quartz with increasing pyrolysis temperatures.<sup>14</sup> Commonly, with increasing pyrolysis temperatures under limited oxygen, the inorganic matter starts as chloritized, hydroxylated, or carbonated metals and then transitions to metallic oxides, some of which can be reduced to pure metals because of the strong reducing atmosphere during pyrolysis (Figure 5). By taking advantage of this transformation process during biochar preparation, researchers are able to create magnetic,<sup>31</sup> zerovalent Fe,<sup>33</sup> and zerovalent Cu coated biochars.<sup>120</sup> Under higher pyrolysis temperatures, calcium carbide (CaC<sub>2</sub>), an important starting material for the production of many chemicals, could be manufactured by mixing fine biochars with CaO.<sup>121</sup> Figure 5 gives the mineral speciation of several elements in biochar. Studies on the inorganic phase of biochars are relatively easier to define than the organic phase due to the higher atomic sensitivity of metal atoms for characterization. Still, there are many other metals, species and mixed crystals that remain unknown and require further research.

The functions of inorganic matter in biochars include but not limited to the following: providing magnetism;<sup>31</sup> catalyzing the decomposition of organic pollutants and metals-

involved catalysis reactions;<sup>33,37,120,124–127</sup> and providing pore-forming agents,<sup>128–130</sup> carbon sequestration agents,<sup>35,131,132</sup> slow-release nutrients,<sup>87,88,133–136</sup> heavy metal coprecipitators,<sup>11,103,137–144</sup> and heavy metal stabilizers.<sup>145</sup> Magnetism emanates from the loading of  $\gamma\text{-Fe}_2\text{O}_3$ <sup>31</sup> and the catalysis is from active zerovalent iron or transition metals,<sup>33,37,120,124–127</sup> and pore-forming agents include KOH,  $\text{ZnCl}_2$ , and others.<sup>128–130</sup> The effect of carbon fixation depends on the mineral type. A five year laboratory experiment indicated that 0.5%–8.9% of biochar carbon was mineralized, and manure-derived biochars mineralize faster than plant-derived biochars,<sup>131</sup> whereas copyrolysis with kaolin, calcite ( $\text{CaCO}_3$ ), or calcium dihydrogen phosphate ( $\text{Ca}(\text{H}_2\text{PO}_4)_2$ ) decreases 0.3%–38% loss of carbon from biochars during tests with potassium dichromate oxidation.<sup>132</sup>

By converting the easy-to-dissolve metallic elements to their difficult-to-dissolve species, heavy metals can be stabilized within biochars.<sup>145</sup> In summary, mineral species within the biochar are transformed by the pyrolysis temperature and affect the biochar structure and applications in various ways. However, more knowledge is needed on the dissolution behavior, toxicity, carbon stability, nanoeffects, and possible catalytic ability of inorganic nanoparticles.

### 2.3. The Surfaces.

The surface of biochar is the main interface where many chemical and biological reactions and interactions occur. Knowledge of the biochar surface chemistry has evolved over time (Figure 4). After categorizing the nature of the biochar surface (aliphatic or aromatic), the functional groups on biochar were elucidated.<sup>25</sup> Following that came the discovery of free radicals on the biochar surface.<sup>146</sup> In this section, the surface functional groups, charge, and free radicals are discussed.

**Surface Functional Groups.**—Characterizing the surface functional groups of biochars can explain their surface chemistry and reactions. Besides aliphatic and aromatic groups, surfaces may include hydroxyl, epoxy, carboxyl, acyl, carbonyl, ether, ester, amido, sulfonic, and azyl groups. Characterization methods have been applied to analyze these functional groups, such as solid-state  $^{13}\text{C}$  NMR,<sup>147</sup> FT-IR,<sup>148</sup> X-ray photoelectron spectroscopy (XPS),<sup>149</sup> and C-1s near-edge X-ray absorption fine structure spectroscopy (NEXAFS).<sup>149–153</sup> Although there are many different types of functional groups and advanced technology for the analysis of functional groups, the precise characterization to distinguish all functional groups was still difficult.

To simplify this process, some studies have focused on surface phenolic–OH, carboxyl, carbonyl, and ester groups as functional groups on biochars.<sup>101,154</sup> These are among the most abundant functional groups at the surface of biochars.<sup>149,154</sup> Another reason is that these functional groups can associate/dissociate with protons in the environment, thus leading to hydrogen bond-induced sorption,<sup>59,143,155–157</sup> biochar alkalis,<sup>23</sup> pH buffering,<sup>158</sup> hydrophilicity/hydrophobicity, surface charge alterations, a cation exchange capacity (CEC),<sup>158</sup> and capacitance improvement.<sup>159</sup> Consequently, defining the dissociation constants ( $\text{p}K_a$ ) and the contents of these functional groups become vital to understanding the surface properties of biochars. Boehm titration methods have been widely applied to measure the

carboxylic acid fraction, lactonic group fraction, and phenolic functional groups for organic materials by  $\text{NaHCO}_3$ ,  $\text{Na}_2\text{CO}_3$ , and  $\text{NaOH}$ , respectively.<sup>160–162</sup> This method offers an easy way to measure different functional groups without knowing their  $\text{p}K_a$  values.

Recently, we proposed an integrated method combining FT-IR and a modified acid/base consuming model to quantitatively identify the chemical states, dissociation constants ( $\text{p}K_a$ ), and contents of surface functional groups within dairy manure-derived biochars.<sup>25</sup> This model offers a method to quantify the contents of different functional groups, but it still requires further investigation to improve the detection accuracy and parameter-fitting results due to the complexity of biochars.

Surface functional groups vary greatly with pyrolysis temperature. The original lignocellulose H-bond networks in biomass were removed, and free hydroxyls were transformed into carboxyls during the pyrolysis process.<sup>163</sup> FT-IR indicated that oxygen-containing groups decreased markedly with increasing pyrolysis temperatures.<sup>10,164</sup> Two-dimensional (2D)  $^{13}\text{C}$  NMR data showed that carbonization resulted in a dehydroxylation/dehydrogenation and aromatization process, along with cleavage of O-alkylate and aromatic O–C–O groups as well as the formation of aromatic C–O groups.<sup>43</sup>

The functional groups on biochar not only served as sorption sites for metal cations<sup>26,50,155,157,165</sup> and ionizable organic pollutants<sup>166,167</sup> but also provided a perfect and cheap active site for the surface chemistry modification of biochar, including oxidation,<sup>60</sup> amination,<sup>168</sup> and sulfonation.<sup>98</sup> For example, the oxidation of biochar can induce more carboxyl groups after soil aging<sup>149</sup> or treatment with hydrogen peroxide.<sup>60</sup> The amino-modification of biochar enhanced the sorption of copper ions.<sup>168</sup> Additionally, sulfonation increased the stearic acid esterification speed of pine pellet biochar.<sup>98</sup> Other studies have reported the introduction of sulfonic acid as benefiting the solubility of carbon materials.<sup>29</sup> As a vital part of the biochar surface, functional groups are important interfacial sites, and more studies are required to quantify them, their contents, their chemical states, and their corresponding applications.

**Surface Charge.**—We are lacking sufficient knowledge of the surface charge on biochars. The surface charge makes biochar attractive or repulsive to other charged molecules<sup>24,169</sup> and bacteria,<sup>170</sup> forming an electrical double layered structure. Thus, biochars display colloidal properties similar to the properties of soil. The origin of the surface charge on biochars is believed to be its aliphatic/aromatic surface and the dissociation of functional groups, such as carboxyl moieties.<sup>163</sup> Therefore, the surface charge of biochars is highly correlated to the pH in the aqueous phase. It remains negative over the natural pH range (pH = 4–12), but in strongly acidic systems, the surfaces of biochars are positively charged. Once the pH increases above a pH of 4, the surfaces of biochars become more negatively charged.<sup>171</sup> Nonetheless, electrostatic interactions impact the transport of ions, nanoparticles, and biochar particles.<sup>172</sup> This influence is strongly regulated by the solution pH.

**Surface Free Radicals.**—In 2014, Liao et al. published a comprehensive description of the biochar's surface free radicals of biochars.<sup>173</sup> They reported abundant and quite persistent free radicals within biochars derived from corn stalks, rice and wheat straws as

observed by electron paramagnetic resonance (EPR).<sup>173</sup> The radical species transitioned from oxygen-centered radicals to carbon-centered and oxygen-centered combined radicals with increasing pyrolysis temperatures.<sup>173</sup> Free radicals can be generated during the charring process.<sup>173–175</sup> Free radical transitions were monitored via in situ EPR observations.<sup>173</sup> Aromatic carbon atoms played an important role in stabilizing the surface free radicals due to their electron-rich aromatic surface at high pyrolysis temperatures.

Although it is difficult to know the specific structures of all free radicals, phenoxy and semiquinone radicals were typically assumed to be the oxygen-centered radicals.<sup>173</sup> Strong ·OH radicals in the aqueous phase were induced by free radicals in biochars. The free radicals in biochars may be a major reason for the inhibition of the germination of plant seeds, root and shoot growth retardation, and damage to the plasma membrane.<sup>173</sup> Other studies indicated that abundant free radicals on the biochar surface could react to activate hydrogen peroxide,<sup>146</sup> persulfate<sup>176</sup> and benefit the degradation of organic contaminants, such as 2-chlorobiphenyl,<sup>146</sup> diethyl phthalate<sup>177</sup> and polychlorinated biphenyls.<sup>176</sup> Free radicals within biochars may be the reason for the electron accepting capacity in high temperature pyrolysis-derived biochars, as measured by mediated electrochemical analysis.<sup>178</sup> Surface radicals on biochars are essential reactive sites, and more attention to their persistence, toxicity, pollutant degradation ability, and environmental impact should be paid.

#### 2.4. Molecular Structures.

**Extracted Small Compounds.**—As one part of biochar molecules, the extracted small compounds have received much attention due to their high mobility and possible toxicity. It was reported that the released fraction from two softwood pellets-derived biochars with high volatile organic compounds (VOCs) almost completely inhibited 94% and 100% of cress seed germination under 5% biochar treatment.<sup>179</sup> After excluding the effects of salt and water stress, researchers believed that the mobile organic compounds were responsible for the adverse effects on germination.<sup>180</sup> However, it is still unclear which compounds are responsible, although phenolic compounds are the leading suspect.<sup>180</sup> Additionally, full identification remains a big challenge due to their low concentration on biochars, lack of viable extraction methods, and theoretical limitation for interpreting mass spectral results. Even if these compounds could be identified, quantification becomes difficult due to the lack of standards and low concentrations. In that case, using a similar compound as a standard or applying relative contents calculated from the peak area could be compromise methods.<sup>181,182</sup>

The extraction of small molecules from different biochars is reported in Table S1.<sup>183–190</sup> Regarding content analysis of the compounds, the depolymerization and C3-side chain shortening occurred at approximately 200–300 °C. The demethoxylation of syringyl and gualacyl lignins appeared at 300–400 °C; dehydroxylation and demethoxylation to remove methoxyl groups appeared at 350–400 °C; complete dehydroxylation of lignin and other biopolymers occurred at 400–500 °C; condensation into aromatic clusters occurred at 300–500 °C; and the partial removal of alkyl bridges between aromatic moieties occurred at 450–500 °C.<sup>182</sup> The related results showed that short carbon chain aldehydes, furans and ketones were the major adsorbed VOCs on biochars pyrolyzed below 350 °C, whereas

adsorbed aromatic compounds and longer carbon chain hydrocarbons dominated in biochars produced under 350 °C.

Regardless of the impact of the pyrolysis temperature, gasified biochars contained higher polycyclic aromatic hydrocarbons (PAHs) and more bioavailable PAHs than produced by fast pyrolysis, which were generally less than biochars derived at slow pyrolysis temperatures.<sup>185</sup> Normally, the total PAH content within a biochar was ~60 mg kg<sup>-1</sup>, which also depends on the type of precursors. For example, biochars produced from rice husks contained 64 mg total PAHs/kg, whereas wood biochar produced 9.5 mg kg<sup>-1</sup> PAH.<sup>189</sup> Hydrothermally carbonized plant materials displayed much higher VOC contents (0.2–1.6 wt %), including benzenic, phenolic and furanic volatiles along with other aldehydes and ketones.<sup>183</sup> Mostly, the total PAHs refers to the 16 USEPA PAHs, which are considered toxic and persistent. They generally decrease with increasing pyrolysis time and temperature,<sup>185</sup> and some researchers suggested that the solvent-extractable PAH concentrations in biochars reach a peak concentration at a pyrolysis temperature between 400 and 500 °C.<sup>187,191</sup> However, some researchers argued that the total PAHs extracted from biochars are quite low in most cases, and they are below the existing environmental quality standards (maximum acceptable concentration of 8 mg kg<sup>-1</sup> for Norway).<sup>184,185</sup>

The conversion of sewage sludge containing noticeable PAHs to biochar could greatly reduce the PAH content,<sup>190</sup> and the addition of biochar could adsorb the dissolved PAHs from sewage sludge.<sup>192</sup> Thermal drying at 100, 200, and 300 °C can greatly reduce the PAH concentrations of biochar within 24 h at the levels of 33.8–88.1%, >93.3%, and >97%, respectively.<sup>188</sup> In addition, blending with low VOC biochar (containing 90% low VOC biochar) was effective in reducing the toxicity of small compounds by at least 50%, whereas simple open-air storage was insufficient.<sup>179</sup> In short, the extraction of small compounds comprised only a small part of the total biochar mass (generally <5%), whereas a large fraction of the small molecules in biochar remain unknown. The mobility, toxicity, concentration, and bioavailability are the main questions regarding these small compounds extracted from biochars. Whether biochar is a source or sink for small extracted compounds and the role of these compounds in the formation of surface radicals remain unclear.

**Skeletal Structures and Models of Biochars.**—The small compounds extracted from biochars differ depending on various precursors (Table S1) and pyrolysis temperatures. However, the small extracted molecules comprise only a small part of biochar mass, less than one-hundredth. Thus, a large amount of biochar mass remains nonextractable and unknown. Theoretically, the unextracted fraction of biochars should contain larger molecular weight compounds and stronger chemical bonds than the extracted compounds and are thus difficult to detect. As it contains heterogeneous structures, biochar is postulated to contain multiple molecules with different molecular weights following the Gaussian distribution law,<sup>21</sup> similar to the molecular weight distribution in polymers. Therefore, the research focus of biochar structures should consider both the entirety of the structure and small-scale features. Studying the extracted small compounds will benefit the understanding of reactions and properties at the micro- and nanoscales. Meanwhile, an integrated and skeletal structural view will help to elucidate the heterogeneous structures of biochars and will assist in the

modification, engineering, and application of biochars for solving new problems, especially as we begin to see their potential as integrated global materials.

To investigate the skeletal structures of biochars, solid  $^{13}\text{C}$  NMR, Raman spectroscopy, and the H/C atomic ratio were applied. Understanding biochar skeletal structures evolved from a hypothesis to a calculated structure to an actual observation (Figure 4). According to the ideal development of biochar structures proposed by Downie et al.,<sup>1</sup> the skeletal carbon within biochars experienced amorphous aromatic carbon, conjugated aromatic carbon, and graphitic carbon successively with increasing pyrolysis temperatures.<sup>1</sup> Later on, Brewer et al. characterized the structures of biochars from fast pyrolysis and gasification, and they proposed aromatic cluster models of these biochars calculated by quantitative  $^{13}\text{C}$  NMR.<sup>119</sup> The skeletal structures of the chars in *Terra Preta* soils were analyzed by quantitative  $^{13}\text{C}$  NMR spectroscopy and were shown to have ~6 fused aromatic rings with abundant  $\text{COO}^-$  groups. Recently, we proposed a simplified method to calculate the fused aromatic clusters of biochars derived from different pyrolysis temperatures by the H/C atomic ratios according to the rectangle-like polycyclic aromatic ring model.<sup>22</sup> The aromatic cluster structures of biochars derived at pyrolysis temperatures of 500 and 700 °C were further calculated as owning  $5 \times 5$  and  $10 \times 10$  rectangle-like polycyclic aromatic structures with the aromatic cluster sizes of  $1.25 \text{ nm} \times 1.25$  and  $2.5 \text{ nm} \times 2.5$  nm, respectively.<sup>22</sup> In addition, the H/C atomic ratio could also act as a smart linkage to build a quantitative relationship based on the pyrolysis temperatures, aromatic clusters, and sorption properties of biochars, as summarized from published and unpublished data from worldwide laboratories with diverse precursor materials.<sup>22</sup> Afterward, an observation of clear aromatic clusters within biochars was reported by applying high-resolution transmission electron microscopy.<sup>21</sup>

The Stone–Wales transformation was also first reported in biochar,<sup>21</sup> which is possibly the reason why fullerenes can be found in the natural environment.<sup>193</sup> These studies provide an integrated and skeletal structure in view of aromatic clusters especially attributed to biochars produced under high pyrolysis temperatures. Although alkyl moieties may coexist with the aromatic clusters in the high pyrolysis temperatures-derived biochars,<sup>147</sup> the hypothesized and observed aromatic structures of biochars provide a simplified and integrated structural model by considering biochar as a whole. These models do not deny the existence of other small compounds though, either internal to biochar or on the surface. We recognize that further studies are still needed to improve the structure to account for more varied observations. In addition, challenges remain to understand typical skeletal structures for biochars derived at middle pyrolysis temperatures.

### 3. BIOCHAR APPLICATIONS

#### 3.1. Carbon Sequestration in Soil.

In the field of climate, the most important application of biochar is to capture the carbon and store it in biochar amended soils, which makes the stability of biochar essential for the control of climate change and for implementing negative GHG emissions. Measuring the carbon stability of biochars is key to evaluating carbon fixation.

Five different evaluation methods have been proposed to measure carbon stability in biochars including the following: the H/C atomic ratio method<sup>194</sup> as well as physical,<sup>195</sup> chemical,<sup>194,196</sup> biological,<sup>197</sup> and thermodynamic methods.<sup>198</sup> The H/C atomic ratio is considered to be an index of the aromaticity of biochars due to hydrogenation and dehydrogenation processes,<sup>22</sup> and the O/C atomic ratio refers to the oxidative degree of biochars due to oxidation or reduction processes.<sup>27,55,56,58,199</sup> Elemental ratios offer an easy first-approximation to evaluate the integral properties and carbon stability of biochar. Nevertheless, it is worth noting that the elemental analysis may not be accurate when other elements (such as S, P, Cl,...) are ignored, and this inaccuracy becomes even larger when oxygen is determined indirectly by weight difference.<sup>22</sup> Physical processes generally refer to the disintegration process due to frost, temperature, and moisture changes; salt weathering; root stress; or mechanical stress through tillage.<sup>200</sup> They are not widely used<sup>195</sup> because of the low carbon loss and because no standard physical method is available for carbon stability evaluations. Several studies propose physical methods to imitate natural weathering processes by repeated wetting/drying and freezing/thawing.<sup>57,201</sup> Biological carbon stability is highly related to the types of biochar, microbes and soils,<sup>197,202</sup> making the results somewhat variable and uncertain. It is conducted by incubating biochars with soils for many days.<sup>57,201</sup>

Chemical evaluation is the most popular method to measure carbon stability, which can be differentiated into the H<sub>2</sub>O<sub>2</sub> and the dichromate method. In the H<sub>2</sub>O<sub>2</sub> method, 0.1 g of biochars is treated with 7 mL of 5% H<sub>2</sub>O<sub>2</sub> at 80 °C for 48 h, and the stable carbon is reported as the percentage of the initial 0.1 g biochar that remains after the reaction.<sup>194</sup> Borrowed from the national environmental protection standard of China related to soil organic matter (SOM), Chen et al.<sup>196</sup> proposed a dichromate method to test biochar carbon stability, described as 0.15 g of biochar added to 55 mL of 0.1 M K<sub>2</sub>Cr<sub>2</sub>O<sub>7</sub> and 11 M H<sub>2</sub>SO<sub>4</sub> and heated at 135 °C for 30 min. The carbon remaining is regarded as stable carbon. Other modified dichromate methods have also been reported.<sup>201,203</sup> As for thermal carbon stability, in 2012, Harvey et al.<sup>198</sup> reported an index, a ratio of the temperatures of biochar to graphite, where 50% of the weight of the organic matter was lost (ash-correction was needed) under thermogravimetric analysis using a 10 mL min<sup>-1</sup> air flow.

Of course, the application of biochar for carbon sequestration is not only a matter of stabilizing the carbon within the biochar itself but also the mass of carbon that the biochar could remove from the atmosphere. For example, the uptake of CO<sub>2</sub> was reported as 73.55 mg g<sup>-1</sup> at 25 °C for biochar produced from sugar cane bagasse at 600 °C.<sup>204</sup> Regardless, the impact on the soil carbon sink should be evaluated after biochar is added into the soil. The clay in the soil could benefit carbon stability in biochars due to the protection of carbon from microbial decomposition.<sup>205</sup> Carbon mineralization of biochars can be influenced by the type of soil.<sup>70,206</sup> Variables include the growth of plant carbon and vegetation, SOM, microbial carbon in the soil, GHG, and atmospheric carbon dioxide concentrations (Figure 6). The addition of biochars to soils affects carbon sinks and sources, but mostly, the biochar acts as a carbon sink for CO<sub>2</sub> from the atmosphere, which is stored in the soil. In turn, the biochar may cause plants and microbes to grow better and store more carbon, increasing the SOM, and CO<sub>2</sub> in the soil.

Regarding plant carbon, it is reported that the addition of 4% straw-derived biochar to soil increased ryegrass production by 68% compared to the control.<sup>207</sup> Although many short-term positive effects of biochars on plant growth were reported,<sup>208,209</sup> there were few statistically significant positive results in long-term experiments.<sup>210</sup> However, statistically, a meta-analysis composed of 177 individual studies indicated an average increase in crop productivity of approximately 10% with the addition of biochar.<sup>17</sup> Another recent meta-analysis of 371 independent studies from 114 published papers revealed a similar positive effect of biochar addition on crop productivity.<sup>96</sup> As for the effect of biochar on SOM mineralization, contrary effects (such as stimulating (known as the “positive priming effect”),<sup>211,212</sup> suppressing (known as the “negative priming effect”),<sup>118,213,214</sup> and no effect<sup>215,216</sup>) were reported.<sup>217,218</sup> A meta-analysis of 650 data points from 18 studies revealed an average positive priming effect of 0.3 mg C g<sup>-1</sup> soil on the SOM, and this priming effect decreased with time.<sup>217</sup>

The labile fraction may also trigger the activity of soil microorganisms in the short term,<sup>217</sup> and a higher dissolved organic carbon flux was observed in one study.<sup>219</sup> Over the long-term, the positive priming effect will decrease or even turn into a negative priming effect due to physical protection mechanisms by adsorbing organic matter onto the biochar surface or into microaggregates.<sup>217,220,221</sup> In fact, much of the variation of the SOM with the addition of biochar can be explained by the activities of the soil microbial community.<sup>222</sup> The impact of biochar on soil microbes depends on the precursors of the biochar and soil type. Steinbeiss et al. stated that the yeast-derived biochar can promote fungal microorganisms, whereas glucose-derived biochar can be utilized by Gram-negative bacteria in soil.<sup>223</sup> The application of biochar increased the bacterial biomass in flinty clay loam soil, especially the abundance of Gram-negative bacteria and Actinobacteria.<sup>84</sup> Meanwhile, for coarse textured soils, the addition of biochar decreased the microbial community.<sup>224</sup>

Other functions of biochars are providing nutrients or acting as conductive carbon materials due to their aromatic structures, which enhances the metabolism of microorganisms.<sup>225–227</sup> Moreover, biochar can also be the habitat for immobilized bacteria to enhance the bioremediation of PAH-contaminated soil.<sup>228</sup> GHGs in soils may be affected by the addition of biochar. These can be divided into CO<sub>2</sub> and non-CO<sub>2</sub> gases, which usually refer to CH<sub>4</sub> and N<sub>2</sub>O. As a GHG, CH<sub>4</sub> is 23 times and N<sub>2</sub>O is several hundred times more potent than CO<sub>2</sub>.<sup>229</sup> Biochar was reported to reduce GHGs emission by approximately 37–91.2% in most cases.<sup>229–234</sup> On the other hand, a few studies reported no obvious reduction<sup>235</sup> or even a 100% increase in CO<sub>2</sub> emissions from soils as a result of the addition of biochar.<sup>236</sup>

The weathering process can greatly weaken the function of fresh biochars in reducing GHG emissions.<sup>237</sup> According to real-time quantitative polymerase chain reaction (qPCR), the mechanism of the CH<sub>4</sub> emission reductions in the presence of biochar in Chinese paddy soils was not the inhibition of methanogenic archaeal growth but rather the 3–7 times increase in the abundance of methanotrophic proteobacterial as well as a decrease in the ratio of methanogenic to methanotrophic abundances (from 36.2% to 4.0%–5.3%).<sup>238</sup>

Rather than focusing on the impact of biochars to a single carbon sink, full-scale assessments, such as life cycle assessments of biochar on soil carbon systems, are needed. It



was reported that the addition of biochar to soils has a carbon abatement potential,<sup>239</sup> and the biochars obtained through slow pyrolysis show the best carbon abatement performance.<sup>240</sup> However, after analyzing the energetic, economic, and climate change potential, researchers are still concerned that biochar only delivers climate change mitigation benefits, whereas the economic viability still remains unclear, and the need for proper waste management shows a greater potential for economic profitability.<sup>241</sup>

The relationships between the structures and carbon stability of biochars could be interpreted from their elements, phases, surfaces, and molecules. The species and content of carbon are certainly two of the most important factors that determine biochar carbon fixation. As for the phases, the loading of the inorganic phase has a great effect on biochar carbon stability.<sup>108</sup> It has been reported that some special structures between the organic and inorganic phases (such as the core-shell C-Si phase structure) may influence the carbon stability of biochars,<sup>14,52</sup> suggesting that the precursor structures can be an important way to improve biochar carbon sequestration. The surface charge and surface free radicals of biochars prevented microbes from attaching and mineralizing on the carbon structure, thus making biochars less bioavailable and enhancing carbon stability. The loss of small extracted molecules and the oxidation of skeletal carbon molecules are vital ways to lose carbon. Molecular computer calculations can be utilized to distinguish the labile functionalized carbon type. In summary, to evaluate the effect of the addition of biochar to soils on climate change, many studies have included stability assessment methods, analyzed the impact of biochar toward other GHGs, and evaluated the life cycle of biochar in carbon fixation. However, assessing different biochar structures and their effects on the life cycle assessment are still needed to engineer and design the best biochar.

### 3.2. Fertilizer for Soil.

In the field of agriculture, one of the key applications for biochars is the use of biochar as a fertilizer for plant growth. Unlike traditional fertilizers that could possibly cause serious eutrophication,<sup>242</sup> biochar can be used as a slow-releasing nutrient material, which has been receiving increasing attention. Two major mechanisms endow biochar with the slow-releasing property: unique biochar structures and the sorption-desorption process. For unique biochar structures, the porous network within biochars hinders the release of the nutrients. Unique connections (including the chemical bonding and physical wrapping) of nutrient elements to the carbon materials also leads to slow nutrient release. For example, the silicon dissolution in biochars was reported to protect the carbon structure due to a silicon-carbon wrapping effect.<sup>14</sup> The strong sorption behavior of biochar makes it a perfect naturally formed soil additive to concentrate nutrients in soil and thus allow for slow desorption into the aqueous phase for plant uptake. Many researchers are now taking advantage of this biochar sorption ability to recycle phosphate and other nutrient elements and to hold them in the soil longer.<sup>87</sup> With this property of the slow-release of fertilizers from biochars, the design of biochar for specific nutrient release is vital for agricultural applications, either by loading nutrient species onto biochars or by choosing the right precursors. Multiple precursors offer the possibility for different choices. For example, rice straw is known for its high silicon content;<sup>14</sup> soybean-derived biochar contains a high nitrogen percentage; eggshell-derived biochar has a large amount of calcium,<sup>104</sup> and

manure-derived biochar is rich in mineral content. These various attributes in different precursors allow biochars to be selectively chosen as specific elemental fertilizers. Moreover, the elemental species and structures within biochars have a great effect on biochar fertilizer release. It was reported that silicic acid is much easier to release than crystal silicon within biochars,<sup>14</sup> and nitrogen becomes less available under increasing pyrolysis temperatures resulting from a transformation of  $\text{NH}_4^+$  to heterocyclic-N.<sup>243</sup> Because the recent literature has focused on biochar function as a fertilizer, more information is needed about the release of other nutrients, such as Si, Na, Mg, and some rare elements. Future challenges remain regarding the control of the precise release rate of nutrients by designing proper structures of biochars and by coupling different nutrient elements.

### 3.3. Sorbent for Removing Pollutants.

In the environmental remediation field, sorption is an essential interfacial process that controls the catalysis, transformation, sorption/desorption, fate, and bioavailability of pollutants. Thus, this review seeks to summarize and develop structure-sorption relationships for various biochars and pollutants. Typical pollutants include nonpolar organic pollutants, polar organic pollutants, ionizable organic pollutants, inorganic ions, heavy metals, and gases. The sorption of these pollutants is greatly affected by the biochar structure including the elements, phases, surfaces and molecules. Strong interactions between two elements can be applied for selective pollutant removal, such as the S–Hg bond.<sup>244</sup> The sorption of ionizable pollutants and cationic heavy metals may lead to a hydrogen proton release or adsorption, possibly resulting from H-bonding and/or ionexchange sorption mechanisms.<sup>167</sup>

Phase effects on the sorption of charcoal have been studied for a long time. As shown in Figure 7, we found that the sorption mechanisms of aromatic contaminants by biochars under different pyrolysis temperatures evolved from the dominance of a partitioning behavior at low temperature to an adsorption dominance at high pyrolysis temperatures.<sup>10</sup> The adsorption mechanism of biochar transitioned from polar-selective to pore filling character with increasing pyrolysis temperatures.<sup>10</sup> This transitional sorption mechanism from partitioning to adsorption induced the sorption rate transition from a fast to a slow process and finally back to fast with increasing pyrolysis temperature.<sup>245</sup> This structural transition of biochars further influenced bisolute sorption and the thermodynamic behavior of biochars.<sup>246</sup> In addition, the washing process with water or the deashing process increased the sorption by biochars because of their enhanced hydrophobic sorption sites.<sup>53</sup> Furthermore, the existence of dissolved organic matter will block the micropores and hinder the sorption of biochars.<sup>247</sup>

New phases may be generated in biochars when heavy metals are adsorbed due to a coprecipitation mechanism. For the most-studied heavy metals, a coprecipitation sorption mechanism was widely reported between the metal ions and biochar inorganic phases. Biochar inorganic phases are characterized as containing  $\text{CO}_3^{2-}$ ,  $\text{PO}_4^{3-}$ ,  $\text{SiO}_3^{2-}$ ,  $\text{OH}^-$ , silicon particles,<sup>26</sup>  $\gamma\text{-Fe}_2\text{O}_3$  particles,<sup>248</sup> and  $\text{MnO}_x$  particles,<sup>36</sup> while also forming precipitates such as  $\beta\text{-Pb}_9(\text{PO}_4)_6$ ,<sup>11</sup>  $\text{Pb}_3(\text{CO}_3)_2(\text{OH})_2$ ,<sup>11</sup>  $5\text{PbO}\cdot\text{P}_2\text{O}_5\cdot\text{SiO}_2$ ,<sup>143</sup>  $\text{Cu}_3(\text{CO}_3)_2(\text{OH})_2$ ,<sup>249</sup>  $\text{KAlSi}_3\text{O}$ ,<sup>26</sup>  $\text{CdCO}_3$ ,  $\text{Cd}_3\text{P}_2$ ,  $\text{Cd}_3(\text{PO}_4)_2$ , and  $\text{K}_4\text{CdCl}_6$ .<sup>250</sup>

Surface functional groups are responsible for the surface effect on the sorption of biochars. The dissociation/association of biochar surface functional groups and the ionizable organic pollutants control the H-bond interactions. Many researchers reported a pH-dependent sorption behavior of ionizable organic pollutants.<sup>166,251–254</sup> For the sorption of sulfamethazine onto charcoal, the sorption mechanism was proposed to be a  $\pi^+ - \pi$  donor–acceptor interaction at low pH, and a negative charge-assisted H-bond at high pH ((–)CAHB, Figure 7).<sup>166</sup> A quantitative study on the H-bond interactions is still needed to evaluate the contribution of H-bonding with  $pK_a$  considerations from both biochar functional groups and ionizable pollutants.

As for inorganic pollutants, complexation, electrostatic effects, and coprecipitation are called upon to describe the interactions between metal ions and the surface of biochars (Figure 7). In a sorption study of rice straw-derived biochars toward  $Pb^{2+}$ , low pyrolysis temperature biochars exhibited a higher sorption ability,<sup>255,256</sup> which may be due to abundant oxygen-containing groups and uncrystallized silicon.<sup>157</sup> The highest adsorption for metal cations occurred for low and middle pyrolysis temperature-derived biochars (Figure 7). As for other anionic inorganic pollutants, such as  $F^-$ ,  $ClO_4^-$ ,  $PO_4^{3-}$ , Cr(III), and Cr(VI), they generally exhibited much lower sorption onto biochars due to electrostatic repulsion interactions. Besides electrostatic interactions, H-bonding to oxygen-containing functional groups within biochars could be a dominant mechanism for  $ClO_4^-$  adsorption, and this hydrogen bonding could be enhanced by the aromatic and hydrophobic surfaces of high pyrolysis temperature-derived biochars,<sup>171</sup> leading to the best sorption toward inorganic anions occurring for high pyrolysis temperature-derived biochars (Figure 7).

Regarding molecular effects, only a few researchers have reached this far. In 2016, a structure–sorption relationship between biochar and naphthalene/phenanthrene was proposed after considering the assumed aromatic cluster structures and summarizing dozens of published or unpublished data.<sup>22</sup> This is probably a very important step to build a structure–sorption relationship between biochar molecular structures and various pollutants. Most studies on sorption mechanisms remains at the empirical/observational level. However, understanding at the molecular level is needed to distinguish the contributions of various sorption mechanisms and different fractions of biochars.

### 3.4. Carbon-Based Materials.

Much previous traditional carbon-based material research was focused on activated carbon. The difference between biochars and activated carbon include the following: (1) biochars usually contains mineral constituents, whereas activated carbon does not, and biochar can be considered to be a robust product, while activated carbon was a refined product; (2) the preparation temperature for biochars (<700 °C) is generally lower than that of activated carbon (>800 °C), and biochar preparation does not need an activation process, whereas the preparation of activated carbon does need chemical activation; (3) biochar shows a much lower surface area than activated carbon; and (4) the types of precursors for biochar preparation are much wider than those for activated carbon, making biochar much cheaper than activated carbon. Because of the cheapness and the wide elements of biochars, biochar is more suitable for carbon fixation and as a soil fertilizer. Although activated carbon shows

a higher sorption ability than biochar, a soil remediation project could hardly afford activated carbon as a sorbent, in addition to the fact that other organic matters in the soil may block the pores of activated carbon and thus decrease its sorption ability. Meanwhile, activated carbon is still preferable for rigorous situations such as medicine purification.

Recently, because of the cheap biomass sources, biochars are increasingly considered as carbon-based materials for economically viable and sustainable applications. Chemical modification of biochars and microbial attachment for bioaugmentation are receiving increased attention. Chemical modifications could be designed based on the multilevel structures of biochars. Other elements such as MgO have been loaded onto biochars for phosphate retention<sup>34,87</sup> and CO<sub>2</sub> capture.<sup>35</sup> The additions of magnetic Fe was first reported in 2011 to enhance the sorption performance and to benefit the solid–liquid phase separation of biochars.<sup>31</sup> By inducing sulfuric acid groups onto biochars as functional groups, a biochar-based solid acid catalyst was built for transesterification,<sup>97,98</sup> hydrolysis reactions,<sup>30,99</sup> and biodiesel production.<sup>100,101</sup> Liu et al. has summarized five major directions for biochar modification, including activation, amination, oxidation, sulfonation, and recombination with supported nanostructures.<sup>12</sup> In short, the purpose behind the modification of biochars was to add other properties, such as increasing their sorption ability and attaching nanoparticles, or by loading the catalyst and taking advantage of the aromatic platform on biochar, its functional groups, and/or high surface area.<sup>12,257</sup> Modifications have enriched the applications of biochars, but evaluation of their practicality and stability are lacking. Attached chemicals and nanoparticles may be lost, and feasible applications require more research. Homogeneous carbon structures and special three-dimensional structural designs may be needed to achieve better performance for carbon-based material applications.

Another important application of biochars as carbon-based materials is for microbial growth. By taking advantage of the sorption ability of biochar, for example, the bioremediation ability of *Pseudomonas putida* bacterial strains was enhanced to degrade PAHs by 24%–38% once immobilized onto biochars compared to biomass.<sup>228</sup> The electron shuttle role that biochars can play may benefit *Shewanella* for reduction reactions.<sup>227</sup> Microbial growth on biochars actually combines the merits of both biochars and microbes, where biochars can adsorb but not degrade the pollutants, whereas microbes can then access the contaminant and degrade them. Interactions between biochars and microbes are achieving increasing attention in the agricultural field. In addition, due to the conductive properties of high pyrolysis temperature-derived biochar, biochar could also be used for energy applications as a carbon-based material, such as microbial fuel cells,<sup>258</sup> supercapacitors,<sup>159</sup> electrocoagulation,<sup>259</sup> and other systems.

#### 4. OUTLOOK OF BIOCHAR STRUCTURES AND APPLICATIONS

Extensive research on biochars continues because of their low cost and versatile applications. Multiple biochar sources and multilevel structures as well as their diverse applications have created many opportunities. We summarize several aspects of biochar structures and applications in Figure 8. Similar to the multilevel discussion in this review, the studies on biochar structures should evolve from the bulk, to the surface and finally to

the molecular scale. Applications for biochar include carbon fixation, soil improvement, and novel carbon-based materials as soil additives including fertilizers, sorbents, and the bioaugmentation of microbes. Regarding the biochar structure, a deeper understanding is expected on the functions, mobility, toxicity, concentration, bioavailability, and environmental fate of phases, surface radicals, and molecules. Furthermore, the development of standard methods will be needed, including but not limited to the following: the quantification and identification of different species, phases, surfaces, and molecules of varying molecular weights in biochars, standard extraction procedures, standard methods for the exfoliation of biochars, and standard comparison methods.

For applications, the deeper our understanding of the structure–application relationships, the better we can choose and design biochars. As shown in Figure 8, the relationships between the structure and application of biochars are gradually improving from qualitative to semiquantitative and finally to quantitative relationships. Although some of these relationships have been previously explored, much research remains related to the structure–application relationships, especially for molecular structural relationships. Phenomena have been reported where one property impacts an application behavior, but seldom do we know the underlying mechanism, and we can never predict a quantitative relationship. On the basis of the interpretation of biochar structures in this review, we recommend that studies on biochars should combine at both the macroscopic and the microscopic levels, while distinguishing both causes and effects. For example, when considering the fate of biochars in soil systems, research should report the release of total elements (including carbon), and the effects on biochar-nanoparticles, the dissolved biochar phase, extracted molecules, and the skeletal biochar structure. When considering biochar toxicity, the persistent free radicals, trace heavy metals, small extracted molecules, and main skeletal molecules of biochars should be investigated. More attention should be paid to linking the structures of biochar with its applications based on fundamental underlying mechanisms. Precise and quantitative predictions of different biochars with various structures for various applications are needed. We anticipate the intelligent design of biochars to achieve the greatest agricultural and environmental benefits possible.

## Supplementary Material

Refer to Web version on PubMed Central for supplementary material.

## ACKNOWLEDGMENTS

This project was supported by the National Natural Science Foundations of China (Grant 21621005, 21537005, and 21425730), and the National Basic Research Program of China (Grant 2014CB441106), and the National Key Technology Support Program of China (Grant 2015BAC02B01). JLS funding for this research was provided by the U.S. National Institute of Environmental Health Science (NIEHS), Iowa Superfund Research Program Grant No. P42ES013661, and the Center for Global and Regional Environmental Research, University of Iowa.

## REFERENCES

- (1). Lehmann J; Joseph S Biochar for Environmental Management: Science and Technology; Earthscan: Sterling, VA, 2009.
- (2). Shi Y China's resources of biomass feedstock. Eng. Sci 2011, 13 (2), 16–23.

- (3). Meng J; Chen W Biochar in China: Status quo of research and trend of industrial development. *J. Shenyang Agric. Univ. (Social Sciences Edition)* 2013, 15 (1), 1–5.
- (4). Gwenzi W; Chaukura N; Mukome FND; Machado S; Nyamasoka B Biochar production and applications in sub-Saharan Africa: Opportunities, constraints, risks and uncertainties. *J. Environ. Manage* 2015, 150, 250–261. [PubMed: 25521347]
- (5). Akolgo GA; Essandoh EO; Gyamfi S; Atta-Darkwa T; Kumi EN; Maia CMBD The potential of a dual purpose improved cookstove for low income earners in Ghana - Improved cooking methods and biochar production. *Renewable Sustainable Energy Rev.* 2018, 82, 369–379.
- (6). Marris E Putting the carbon back: Black is the new green. *Nature* 2006, 442 (7103), 624–626. [PubMed: 16900176]
- (7). De Gisi S; Petta L; Wendland C History and technology of Terra Preta sanitation. *Sustainability* 2014, 6 (3), 1328–1345.
- (8). Lehmann J A handful of carbon. *Nature* 2007, 447 (7141), 143–144. [PubMed: 17495905]
- (9). Woolf D; Amonette JE; Street-Perrott FA; Lehmann J; Joseph S Sustainable biochar to mitigate global climate change. *Nat. Commun* 2010, 1, 56. [PubMed: 20975722]
- (10). Chen B; Zhou D; Zhu L Transitional adsorption and partition of nonpolar and polar aromatic contaminants by biochars of pine needles with different pyrolytic temperatures. *Environ. Sci. Technol* 2008, 42 (14), 5137–5143. [PubMed: 18754360]
- (11). Cao X; Ma L; Gao B; Harris W Dairy-manure derived biochar effectively sorbs lead and atrazine. *Environ. Sci. Technol* 2009, 43 (9), 3285–3291. [PubMed: 19534148]
- (12). Liu W; Jiang H; Yu H Development of biochar-based functional materials: Toward a sustainable platform carbon material. *Chem. Rev* 2015, 115 (22), 12251–12285. [PubMed: 26495747]
- (13). Meyer S; Glaser B; Quicker P Technical, economical, and climate-related aspects of biochar production technologies: A literature review. *Environ. Sci. Technol* 2011, 45 (22), 9473–9483. [PubMed: 21961528]
- (14). Xiao X; Chen B; Zhu L Transformation, morphology, and dissolution of silicon and carbon in rice straw-derived biochars under different pyrolytic temperatures. *Environ. Sci. Technol* 2014, 48 (6), 3411–3419. [PubMed: 24601595]
- (15). Kozbial A; Zhou F; Li Z; Liu H; Li L Are graphitic surfaces hydrophobic? *Acc. Chem. Res* 2016, 49 (12), 2765–2773. [PubMed: 27935273]
- (16). Atkinson CJ; Fitzgerald JD; Hipsley NA Potential mechanisms for achieving agricultural benefits from biochar application to temperate soils: A review. *Plant Soil* 2010, 337 (1–2), 1–18.
- (17). Jeffery S; Verheijen FGA; van der Velde M; Bastos AC A quantitative review of the effects of biochar application to soils on crop productivity using meta-analysis. *Agric., Ecosyst. Environ* 2011, 144 (1), 175–187.
- (18). Ahmad M; Rajapaksha AU; Lim JE; Zhang M; Bolan N; Mohan D; Vithanage M; Lee SS; Ok YS Biochar as a sorbent for contaminant management in soil and water: A review. *Chemosphere* 2014, 99, 19–33. [PubMed: 24289982]
- (19). Inyang MI; Gao B; Yao Y; Xue YW; Zimmerman A; Mosa A; Pullammanappallil P; Ok YS; Cao XD A review of biochar as a low-cost adsorbent for aqueous heavy metal removal. *Crit. Rev. Environ. Sci. Technol* 2016, 46 (4), 406–433.
- (20). Devi P; Saroha AK Utilization of sludge based adsorbents for the removal of various pollutants: A review. *Sci. Total Environ* 2017, 578, 16–33. [PubMed: 27838056]
- (21). Xiao X; Chen B A direct observation of the fine aromatic clusters and molecular structures of biochars. *Environ. Sci. Technol* 2017, 51 (10), 5473–5482. [PubMed: 28399630]
- (22). Xiao X; Chen Z; Chen B H/C atomic ratio as a smart linkage between pyrolytic temperatures, aromatic clusters and sorption properties of biochars derived from diverse precursory materials. *Sci. Rep* 2016, 6, 22644. [PubMed: 26940984]
- (23). Yuan J; Xu R; Zhang H The forms of alkalis in the biochar produced from crop residues at different temperatures. *Bioresour. Technol* 2011, 102 (3), 3488–3497. [PubMed: 21112777]
- (24). Xu Y; Chen B Organic carbon and inorganic silicon speciation in rice-bran-derived biochars affect its capacity to adsorb cadmium in solution. *J. Soils Sediments* 2015, 15 (1), 60–70.

- (25). Chen Z; Xiao X; Chen B; Zhu L Quantification of chemical states, dissociation constants and contents of oxygen-containing groups on the surface of biochars produced at different temperatures. *Environ. Sci. Technol* 2015, 49 (1), 309–317. [PubMed: 25453912]
- (26). Qian L; Chen B Dual role of biochars as adsorbents for aluminum: The effects of oxygen-containing organic components and the scattering of silicate particles. *Environ. Sci. Technol* 2013, 47 (15), 8759–8768. [PubMed: 23826729]
- (27). Spokas KA Review of the stability of biochar in soils: Predictability of O:C molar ratios. *Carbon Manage.* 2010, 1 (2), 289–303.
- (28). Rondon MA; Lehmann J; Ramirez J; Hurtado M Biological nitrogen fixation by common beans (*Phaseolus vulgaris* L.) increases with bio-char additions. *Biol. Fertil. Soils* 2007, 43 (6), 699–708.
- (29). Zhao G; Jiang L; He Y; Li J; Dong H; Wang X; Hu W Sulfonated graphene for persistent aromatic pollutant management. *Adv. Mater* 2011, 23 (34), 3959–3963. [PubMed: 21800380]
- (30). Ormsby R; Kastner JR; Miller J Hemicellulose hydrolysis using solid acid catalysts generated from biochar. *Catal. Today* 2012, 190 (1), 89–97.
- (31). Chen B; Chen Z; Lv S A novel magnetic biochar efficiently sorbs organic pollutants and phosphate. *Bioresour. Technol* 2011, 102 (2), 716–723. [PubMed: 20863698]
- (32). Xiao X; Chen B; Zhu L; Schnoor JL Sugar cane-converted graphene-like material for the superhigh adsorption of organic pollutants from water via coassembly mechanisms. *Environ. Sci. Technol* 2017, 51 (21), 12644–12652. [PubMed: 29016116]
- (33). Yan J; Han L; Gao W; Xue S; Chen M Biochar supported nanoscale zerovalent iron composite used as persulfate activator for removing trichloroethylene. *Bioresour. Technol* 2015, 175, 269–274. [PubMed: 25459832]
- (34). Zhang M; Gao B; Yao Y; Xue Y; Inyang M Synthesis of porous MgO-biochar nanocomposites for removal of phosphate and nitrate from aqueous solutions. *Chem. Eng. J* 2012, 210, 26–32.
- (35). Liu W; Jiang H; Tian K; Ding Y; Yu H Mesoporous carbon stabilized MgO nanoparticles synthesized by pyrolysis of MgCl<sub>2</sub> preloaded waste biomass for highly efficient CO<sub>2</sub> capture. *Environ. Sci. Technol* 2013, 47 (16), 9397–9403. [PubMed: 23895233]
- (36). Wang H; Gao B; Wang S; Fang J; Xue Y; Yang K Removal of Pb(II), Cu(II), and Cd(II) from aqueous solutions by biochar derived from KMnO<sub>4</sub> treated hickory wood. *Bioresour. Technol* 2015, 197, 356–362. [PubMed: 26344243]
- (37). Shen Y; Zhao P; Shao Q; Ma D; Takahashi F; Yoshikawa K In-situ catalytic conversion of tar using rice husk char-supported nickeliron catalysts for biomass pyrolysis/gasification. *Appl. Catal., B* 2014, 152, 140–151.
- (38). Wang T; Camps-Arbestain M; Hedley M; Singh BP; Calvelo-Pereira R; Wang CY Determination of carbonate-C in biochars. *Soil Res.* 2014, 52 (5), 495–504.
- (39). Xu Y; Chen B Investigation of thermodynamic parameters in the pyrolysis conversion of biomass and manure to biochars using thermogravimetric analysis. *Bioresour. Technol* 2013, 146, 485–493. [PubMed: 23958681]
- (40). Keiluweit M; Nico PS; Johnson MG; Kleber M Dynamic molecular structure of plant biomass-derived black carbon (biochar). *Environ. Sci. Technol* 2010, 44 (4), 1247–1253. [PubMed: 20099810]
- (41). Chia CH; Gong B; Joseph SD; Marjo CE; Munroe P; Rich AM Imaging of mineral-enriched biochar by FTIR, Raman and SEM-EDX. *Vib. Spectrosc.* 2012, 62, 248–257.
- (42). Jindo K; Mizumoto H; Sawada Y; Sanchez-Monedero MA; Sonoki T Physical and chemical characterization of biochars derived from different agricultural residues. *Biogeosciences* 2014, 11 (23), 6613–6621.
- (43). Li X; Shen Q; Zhang D; Mei X; Ran W; Xu Y; Yu G Functional groups determine biochar properties (pH and EC) as studied by two-dimensional C-13 NMR correlation spectroscopy. *PLoS One* 2013, 8 (6), No. e65949. [PubMed: 23840381]
- (44). Le Brech Y; Delmotte L; Raya J; Brosse N; Gadiou R; Dufour A High resolution solid state 2D NMR analysis of biomass and biochar. *Anal. Chem* 2015, 87 (2), 843–847. [PubMed: 25521946]
- (45). Ma J; Takahashi E *Soil, Fertilizer, and Plant Silicon Research in Japan*; Elsevier Science: Amsterdam, 2002.

- (46). Savant NK; Datnoff LE; Snyder GH Depletion of plantavailable silicon in soils: A possible cause of declining rice yields. *Commun. Soil Sci. Plant Anal* 1997, 28 (13–14), 1245–1252.
- (47). Detmann KC; Araujo WL; Martins SCV; Sanglard LMVP; Reis JV; Detmann E; Rodrigues FA; Nunes-Nesi A; Fernie AR; DaMatta FM Silicon nutrition increases grain yield, which, in turn, exerts a feed-forward stimulation of photosynthetic rates via enhanced mesophyll conductance and alters primary metabolism in rice. *New Phytol.* 2012, 196 (3), 752–762. [PubMed: 22994889]
- (48). Epstein E Silicon: its manifold roles in plants. *Ann. Appl. Biol* 2009, 155 (2), 155–160.
- (49). Keeping MG; Reynolds OL Silicon in agriculture: New insights, new significance and growing application. *Ann. Appl. Biol* 2009, 155 (2), 153–154.
- (50). Qian L; Chen B; Hu D Effective alleviation of aluminum phytotoxicity by manure-derived biochar. *Environ. Sci. Technol* 2013, 47 (6), 2737–2745. [PubMed: 23398535]
- (51). Dai G; Duan M; Wang Z; Zhao Y; Zhu G; Zhou J Study on characteristics of available silicon content in soils in Shaanxi province. *J. Soil Water Conserv* 2004, 18 (5), 51–53.
- (52). Guo J; Chen B Insights on the molecular mechanism for the recalcitrance of biochars: interactive effects of carbon and silicon components. *Environ. Sci. Technol* 2014, 48 (16), 9103–9112. [PubMed: 25017808]
- (53). Sun K; Kang M; Zhang Z; Jin J; Wang Z; Pan Z; Xu D; Wu F; Xing B Impact of deashing reatment on biochar structural properties and potential sorption mechanisms of phenanthrene. *Environ. Sci. Technol* 2013, 47 (20), 11473–11481. [PubMed: 24025082]
- (54). Gilli P; Gilli G Hydrogen bond models and theories: The dual hydrogen bond model and its consequences. *J. Mol. Struct* 2010, 972 (1–3), 2–10.
- (55). Zimmerman AR Abiotic and microbial oxidation of laboratoryproduced black carbon (biochar). *Environ. Sci. Technol* 2010, 44 (4), 1295–1301. [PubMed: 20085259]
- (56). Nguyen BT; Lehmann J; Kinyangi J; Smernik R; Riha SJ; Engelhard MH Long-term black carbon dynamics in cultivated soil. *Biogeochemistry* 2008, 89 (3), 295–308.
- (57). Hale SE; Hanley K; Lehmann J; Zimmerman AR; Cornelissen G Effects of chemical, biological, and physical aging as well as soil addition on the sorption of pyrene to activated carbon and biochar. *Environ. Sci. Technol* 2011, 45 (24), 10445–10453. [PubMed: 22077986]
- (58). Nguyen BT; Lehmann J Black carbon decomposition under varying water regimes. *Org. Geochem* 2009, 40 (8), 846–853.
- (59). Qian L; Chen B Interactions of aluminum with biochars and oxidized biochars: Implications for the biochar aging process. *J. Agric. Food Chem* 2014, 62 (2), 373–380. [PubMed: 24364719]
- (60). Xue Y; Gao B; Yao Y; Inyang M; Zhang M; Zimmerman AR; Ro KS Hydrogen peroxide modification enhances the ability of biochar (hydrochar) produced from hydrothermal carbonization of peanut hull to remove aqueous heavy metals: Batch and column tests. *Chem. Eng. J* 2012, 200, 673–680.
- (61). Knicker H "Black nitrogen" - An important fraction in determining the recalcitrance of charcoal. *Org. Geochem* 2010, 41 (9), 947–950.
- (62). Cantrell KB; Hunt PG; Uchimiya M; Novak JM; Ro KS Impact of pyrolysis temperature and manure source on physicochemical characteristics of biochar. *Bioresour. Technol* 2012, 107, 419–428. [PubMed: 22237173]
- (63). Knicker H; Hilscher A; Gonzalez-Vila FJ; Almendros G A new conceptual model for the structural properties of char produced during vegetation fires. *Org. Geochem* 2008, 39 (8), 935–939.
- (64). Pietrzak R; Wachowska H; Nowicki P Preparation of nitrogen-enriched activated carbons from brown coal. *Energy Fuels* 2006, 20 (3), 1275–1280.
- (65). Pietrzak R; Jurewicz K; Nowicki P; Babel K; Wachowska H Nitrogen-enriched bituminous coal-based active carbons as materials for supercapacitors. *Fuel* 2010, 89 (11), 3457–3467.
- (66). Guo B; Liu Q; Chen E; Zhu H; Fang L; Gong J Controllable N-doping of graphene. *Nano Lett.* 2010, 10 (12), 4975–4980. [PubMed: 20968305]
- (67). Wang T; Arbestain MC; Hedley M; Bishop P Chemical and bioassay characterisation of nitrogen availability in biochar produced from dairy manure and biosolids. *Org. Geochem.* 2012, 51, 45–54.



- (68). Wang Y; Jing X; Li L; Liu W; Tong Z; Jiang H Biototoxicity evaluations of three typical biochars using a simulated system of fast pyrolytic biochar extracts on organisms of three kingdoms. *ACS Sustainable Chem. Eng.* 2017, 5 (1), 481–488.
- (69). Prommer J; Wanek W; Hofhansl F; Trojan D; Offre P; Urich T; Schleper C; Sassmann S; Kitzler B; Soja G; HoodNowotny RC Biochar decelerates soil organic nitrogen cycling but stimulates soil nitrification in a temperate arable field trial. *PLoS One* 2014, 9 (1), No. e86388. [PubMed: 24497947]
- (70). Haefele SM; Konboon Y; Wongboon W; Amarante S; Maarifat AA; Pfeiffer EM; Knoblauch C Effects and fate of biochar from rice residues in rice-based systems. *Field. Crop. Res* 2011, 121 (3), 430–440.
- (71). Lehmann J; Pereira da Silva J, Jr.; Steiner C; Nehls T; Zech W; Glaser B Nutrient availability and leaching in an archaeological Anthrosol and a Ferralsol of the Central Amazon basin: fertilizer, manure and charcoal amendments. *Plant Soil* 2003, 249 (2), 343–357.
- (72.) Schulz H; Glaser B Effects of biochar compared to organic and inorganic fertilizers on soil quality and plant growth in a greenhouse experiment. *J. Plant Nutr. Soil Sci* 2012, 175 (3), 410–422.
- (73). Ding Y; Liu Y-X; Wu W-X; Shi D-Z; Yang M; Zhong Z-K Evaluation of biochar effects on nitrogen retention and leaching in multi-layered soil columns. *Water, Air, Soil Pollut.* 2010, 213 (1–4), 47–55.
- (74). Gai X; Wang H; Liu J; Zhai L; Liu S; Ren T; Liu H Effects of feedstock and pyrolysis temperature on biochar adsorption of ammonium and nitrate. *PLoS One* 2014, 9 (12), No. e113888. [PubMed: 25469875]
- (75). Hale SE; Alling V; Martinsen V; Mulder J; Breedveld GD; Cornelissen G The sorption and desorption of phosphate-P, ammonium-N and nitrate-N in cacao shell and corn cob biochars. *Chemosphere* 2013, 91 (11), 1612–1619. [PubMed: 23369636]
- (76). Hollister CC; Bisogni JJ; Lehmann J Ammonium, nitrate, and phosphate sorption to and solute leaching from biochars prepared from corn stover (*Zea mays* L.) and oak wood (*Quercus* spp.). *J. Environ. Qual* 2013, 42 (1), 137–144. [PubMed: 23673748]
- (77). Yao Y; Gao B; Zhang M; Inyang M; Zimmerman AR Effect of biochar amendment on sorption and leaching of nitrate, ammonium, and phosphate in a sandy soil. *Chemosphere* 2012, 89 (11), 1467–1471. [PubMed: 22763330]
- (78). Taghizadeh-Toosi A; Clough TJ; Sherlock RR; Condon LM Biochar adsorbed ammonia is bioavailable. *Plant Soil* 2012, 350 (1–2), 57–69.
- (79). Spokas KA; Novak JM; Venterea RT Biochar's role as an alternative N-fertilizer: ammonia capture. *Plant Soil* 2012, 350 (1–2), 35–42.
- (80). Xu H; Wang X; Li H; Yao H; Su J; Zhu Y Biochar impacts soil microbial community composition and nitrogen cycling in an acidic soil planted with rape. *Environ. Sci. Technol* 2014, 48 (16), 9391–9399. [PubMed: 25054835]
- (81.) Wang Z; Zheng H; Luo Y; Deng X; Herbert S; Xing B Characterization and influence of biochars on nitrous oxide emission from agricultural soil. *Environ. Pollut* 2013, 174, 289–296. [PubMed: 23291210]
- (82). Luz Cayuela M; Sanchez-Monedero MA; Roig A; Hanley K; Enders A; Lehmann J Biochar and denitrification in soils: When, how much and why does biochar reduce N<sub>2</sub>O emissions? *Sci. Rep* 2013, 3, No. 1732. [PubMed: 23615819]
- (83). Soong JL; Cotrufo MF Annual burning of a tallgrass prairie inhibits C and N cycling in soil, increasing recalcitrant pyrogenic organic matter storage while reducing N availability. *Global Change Biol.* 2015, 21 (6), 2321–2333.
- (84). Prayogo C; Jones JE; Baeyens J; Bending GD Impact of biochar on mineralisation of C and N from soil and willow litter and its relationship with microbial community biomass and structure. *Biol. Fertil. Soils* 2014, 50 (4), 695–702.
- (85). Ngo P-T; Rumpel C; Ngo Q-A; Alexis M; Vargas GV; Gil M. d. I. L. M.; Dang D-K; Jouquet P Biological and chemical reactivity and phosphorus forms of buffalo manure compost, vermicompost and their mixture with biochar. *Bioresour. Technol* 2013, 148, 401–407. [PubMed: 24071441]

- (86). Uchimiya M; Hiradate S Pyrolysis temperature-dependent changes in dissolved phosphorus speciation of plant and manure biochars. *J. Agric. Food Chem* 2014, 62 (8), 1802–1809. [PubMed: 24495088]
- (87). Yao Y; Gao B; Chen J; Yang L Engineered biochar reclaiming phosphate from aqueous solutions: Mechanisms and potential application as a slow-release fertilizer. *Environ. Sci. Technol* 2013, 47 (15), 8700–8708. [PubMed: 23848524]
- (88). Silber A; Levkovitch I; Graber ER pH-dependent mineral release and surface properties of cornstraw biochar: Agronomic implications. *Environ. Sci. Technol* 2010, 44 (24), 9318–9323. [PubMed: 21090742]
- (89). Qian T; Zhang X; Hu J; Jiang H Effects of environmental conditions on the release of phosphorus from biochar. *Chemosphere* 2013, 93 (9), 2069–2075. [PubMed: 23958443]
- (90). Cao X; Ma L; Liang Y; Gao B; Harris W Simultaneous immobilization of lead and atrazine in contaminated soils using dairymanure biochar. *Environ. Sci. Technol* 2011, 45 (11), 4884–4889. [PubMed: 21542567]
- (91). Novak JM; Busscher WJ; Laird DL; Ahmedna M; Watts DW; Niandou MAS Impact of biochar amendment on fertility of a southeastern coastal plain soil. *Soil Sci.* 2009, 174 (2), 105–112.
- (92). Rajkovich S; Enders A; Hanley K; Hyland C; Zimmerman AR; Lehmann J Corn growth and nitrogen nutrition after additions of biochars with varying properties to a temperate soil. *Biol. Fertil. Soils* 2012, 48 (3), 271–284.
- (93). Major J; Rondon M; Molina D; Riha S; Lehmann J Nutrient leaching in a Colombian savanna Oxisol amended with biochar. *J. Environ. Qual* 2012, 41 (4), 1076–1086. [PubMed: 22751049]
- (94). Bird MI; Wurster CM; de Paula Silva PH; Bass AM; de Nys R Algal biochar - production and properties. *Bioresour. Technol* 2011, 102 (2), 1886–1891. [PubMed: 20797850]
- (95). Xu G; Wei LL; Sun JN; Shao HB; Chang SX What is more important for enhancing nutrient bioavailability with biochar application into a sandy soil: Direct or indirect mechanism? *Ecol. Eng* 2013, 52, 119–124.
- (96). Biederman LA; Harpole WS Biochar and its effects on plant productivity and nutrient cycling: A meta-analysis. *GCB Bioenergy* 2013, 5 (2), 202–214.
- (97). Yu JT; Dehkhoda AM; Ellis N Development of biocharbased catalyst for transesterification of canola oil. *Energy Fuels* 2011, 25, 337–344.
- (98). Kastner JR; Miller J; Geller DP; Locklin J; Keith LH; Johnson T Catalytic esterification of fatty acids using solid acid catalysts generated from biochar and activated carbon. *Catal. Today* 2012, 190 (1), 122–132.
- (99). Shen S; Cai B; Wang C; Li H; Dai G; Qin H Preparation of a novel carbon-based solid acid from cocarbonized starch and polyvinyl chloride for cellulose hydrolysis. *Appl. Catal., A* 2014, 473, 70–74.
- (100). Dehkhoda AM; West AH; Ellis N Biochar based solid acid catalyst for biodiesel production. *Appl. Catal., A* 2010, 382 (2), 197–204.
- (101). Rao BVSK; Mouli KC; Rambabu N; Dalai AK; Prasad RBN Carbon-based solid acid catalyst from de-oiled canola meal for biodiesel production. *Catal. Commun* 2011, 14 (1), 20–26.
- (102.) Wang S; Gao B; Li Y; Mosa A; Zimmerman AR; Ma LQ; Harris WG; Migliaccio KW Manganese oxide-modified biochars: Preparation, characterization, and sorption of arsenate and lead. *Bioresour. Technol* 2015, 181, 13–17. [PubMed: 25625462]
- (103). Song Z; Lian F; Yu Z; Zhu L; Xing B; Qiu W Synthesis and characterization of a novel MnO<sub>x</sub>-loaded biochar and its adsorption properties for Cu<sup>2+</sup> in aqueous solution. *Chem. Eng. J* 2014, 242, 36–42.
- (104). Zhao L; Cao X; Wang Q; Yang F; Xu S Mineral constituents profile of biochar derived from diversified waste biomasses: implications for agricultural applications. *J. Environ. Qual* 2013, 42 (2), 545–552. [PubMed: 23673847]
- (105). Lentz RD; Ippolito JA Biochar and manure affect calcareous soil and corn silage nutrient concentrations and uptake. *J. Environ. Qual* 2012, 41 (4), 1033–1043. [PubMed: 22751045]
- (106). Cimo G; Kucerik J; Berns AE; Schaumann GE; Alonzo G; Conte P Effect of heating time and temperature on the chemical characteristics of biochar from poultry manure. *J. Agric. Food Chem* 2014, 62 (8), 1912–1918. [PubMed: 24506474]

- (107). Sun K; Jin J; Keiluweit M; Kleber M; Wang Z; Pan Z; Xing B Polar and aliphatic domains regulate sorption of phthalic acid esters (PAEs) to biochars. *Bioresour. Technol* 2012, 118, 120–127. [PubMed: 22705514]
- (108). McBeath AV; Wurster CM; Bird MI Influence of feedstock properties and pyrolysis conditions on biochar carbon stability as determined by hydrogen pyrolysis. *Biomass Bioenergy* 2015, 73, 155–173.
- (109). Chen Z; Chen B; Zhou D Composition and sorption properties of rice-straw derived biochars. *Acta Scientiae Circumstantiae* 2013, 33 (1), 9–19.
- (110). Chen B; Chen Z Sorption of naphthalene and 1-naphthol by biochars of orange peels with different pyrolytic temperatures. *Chemosphere* 2009, 76 (1), 127–133. [PubMed: 19282020]
- (111). Huang W; Chen B Interaction mechanisms of organic contaminants with burned straw ash charcoal. *J. Environ. Sci* 2010, 22 (10), 1586–1594.
- (112). Dittmar T; Paeng J; Gihring TM; Suryaputra IGNA; Huettel M Discharge of dissolved black carbon from a fire-affected intertidal system. *Limnol. Oceanogr* 2012, 57 (4), 1171–1181.
- (113). Dong X; Ma LQ; Gress J; Harris W; Li Y Enhanced Cr(VI) reduction and As(III) oxidation in ice phase: Important role of dissolved organic matter from biochar. *J. Hazard. Mater* 2014, 267, 62–70. [PubMed: 24418493]
- (114). Jamieson T; Sager E; Gueguen C Characterization of biochar-derived dissolved organic matter using UV-visible absorption and excitation-emission fluorescence spectroscopies. *Chemosphere* 2014, 103, 197–204. [PubMed: 24359913]
- (115). Keith A; Singh B; Singh BP Interactive priming of biochar and labile organic matter mineralization in a smectite-rich soil. *Environ. Sci. Technol* 2011, 45 (22), 9611–9618. [PubMed: 21950729]
- (116). Calvelo Pereira R; Kaal J; Camps Arbestain M; Pardo Lorenzo R; Aitkenhead W; Hedley M; Macias F; Hindmarsh J; Macia-Agullo JA Contribution to characterisation of biochar to estimate the labile fraction of carbon. *Org. Geochem* 2011, 42 (11), 1331–1342.
- (117). Al-Wabel MI; Al-Omran A; El-Naggar AH; Nadeem M; Usman ARA Pyrolysis temperature induced changes in characteristics and chemical composition of biochar produced from conocarpus wastes. *Bioresour. Technol* 2013, 131, 374–379. [PubMed: 23376202]
- (118). Cross A; Sohi SP The priming potential of biochar products in relation to labile carbon contents and soil organic matter status. *Soil Biol. Biochem* 2011, 43 (10), 2127–2134.
- (119). Brewer CE; Schmidt-Rohr K; Satrio JA; Brown RC Characterization of biochar from fast pyrolysis and gasification systems. *Environ. Prog. Sustainable Energy* 2009, 28 (3), 386–396.
- (120). Liu W; Tian K; Jiang H; Zhang X; Ding H; Yu H Selectively improving the bio-oil quality by catalytic fast pyrolysis of heavy-metal-polluted biomass: Take copper (Cu) as an example. *Environ. Sci. Technol* 2012, 46 (14), 7849–7856. [PubMed: 22708628]
- (121). Li G; Liu Q; Liu Z; Zhang ZC; Li C; Wu W Production of calcium carbide from fine biochars. *Angew. Chem., Int. Ed* 2010, 49 (45), 8480–8483.
- (122). Yan Q; Wan C; Liu J; Gao J; Yu F; Zhang J; Cai Z Iron nanoparticles in situ encapsulated in biochar-based carbon as an effective catalyst for the conversion of biomass-derived syngas to liquid hydrocarbons. *Green Chem.* 2013, 15 (6), 1631–1640.
- (123). Sun L; Tian C; Li M; Meng X; Wang L; Wang R; Yin J; Fu H From coconut shell to porous graphene-like nanosheets for highpower supercapacitors. *J. Mater. Chem. A* 2013, 1 (21), 6462–6470.
- (124). Zhou Y; Gao B; Zimmerman AR; Chen H; Zhang M; Cao X Biochar-supported zerovalent iron for removal of various contaminants from aqueous solutions. *Bioresour. Technol* 2014, 152, 538–542. [PubMed: 24300585]
- (125). Zhu X; Liu Y; Qian F; Zhou C; Zhang S; Chen J Preparation of magnetic porous carbon from waste hydrochar by simultaneous activation and magnetization for tetracycline removal. *Bioresour. Technol* 2014, 154, 209–214. [PubMed: 24393746]
- (126). Cheah S; Gaston KR; Parent YO; Jarvis MW; Vinzant TB; Smith KM; Thornburg NE; Nimlos MR; Magrini-Bair KA Nickel cerium olivine catalyst for catalytic gasification of biomass. *Appl. Catal., B* 2013, 134, 34–45.

- (127). Lahijani P; Zainal ZA; Mohamed AR; Mohammadi M CO<sub>2</sub> gasification reactivity of biomass char: Catalytic influence of alkali, alkaline earth and transition metal salts. *Bioresour. Technol* 2013, 144, 288–295. [PubMed: 23880130]
- (128). Azargohar R; Dalai AK Steam and KOH activation of biochar: Experimental and modeling studies. *Microporous Mesoporous Mater.* 2008, 110 (2–3), 413–421.
- (129). Azargohar R; Dalai AK Biochar as a precursor of activated carbon. *Appl. Biochem. Biotechnol* 2006, 131 (1–3), 762–773. [PubMed: 18563652]
- (130). Angin D; Altintig E; Kose TE Influence of process parameters on the surface and chemical properties of activated carbon obtained from biochar by chemical activation. *Bioresour. Technol* 2013, 148, 542–549. [PubMed: 24080293]
- (131). Singh BP; Cowie AL; Smernik RJ Biochar carbon stability in a clayey soil as a function of feedstock and pyrolysis temperature. *Environ. Sci. Technol* 2012, 46 (21), 11770–11778. [PubMed: 23013285]
- (132). Li F; Cao X; Zhao L; Wang J; Ding Z Effects of mineral additives on biochar formation: Carbon retention, stability, and properties. *Environ. Sci. Technol.* 2014, 48 (19), 11211–11217. [PubMed: 25203840]
- (133). Wang T; Camps-Arbestain M; Hedley M; Bishop P Predicting phosphorus bioavailability from high-ash biochars. *Plant Soil* 2012, 357 (1–2), 173–187.
- (134). Tsai W; Liu S; Chen H; Chang Y; Tsai Y Textural and chemical properties of swine-manure-derived biochar pertinent to its potential use as a soil amendment. *Chemosphere* 2012, 89 (2), 198–203. [PubMed: 22743180]
- (135.) Wu H; Yip K; Kong Z; Li C-Z; Liu D; Yu Y; Gao X Removal and recycling of inherent inorganic nutrient species in Mallee biomass and derived biochars by water leaching. *Ind. Eng. Chem. Res* 2011, 50 (21), 12143–12151.
- (136). Yao FX; Arbostain MC; Virgel S; Blanco F; Arostegui J; Macia-Agullo JA; Macias F Simulated geochemical weathering of a mineral ash-rich biochar in a modified Soxhlet reactor. *Chemosphere* 2010, 80 (7), 724–732. [PubMed: 20542316]
- (137). Xu X; Cao X; Zhao L Comparison of rice husk- and dairy manure-derived biochars for simultaneously removing heavy metals from aqueous solutions: Role of mineral components in biochars. *Chemosphere* 2013, 92 (8), 955–961. [PubMed: 23591132]
- (138). Uchimiya M; Klasson KT; Wartelle LH; Lima IM Influence of soil properties on heavy metal sequestration by biochar amendment: 1. Copper sorption isotherms and the release of cations. *Chemosphere* 2011, 82 (10), 1431–1437. [PubMed: 21147495]
- (139). Agrafioti E; Bouras G; Kalderis D; Diamadopoulos E Biochar production by sewage sludge pyrolysis. *J. Anal. Appl. Pyrolysis* 2013, 101, 72–78.
- (140). Ahmad M; Lee SS; Lim JE; Lee S-E; Cho JS; Moon DH; Hashimoto Y; Ok YS Speciation and phytoavailability of lead and antimony in a small arms range soil amended with mussel shell, cow bone and biochar: EXAFS spectroscopy and chemical extractions. *Chemosphere* 2014, 95, 433–441. [PubMed: 24183621]
- (141). Inyang M; Gao B; Ding W; Pullammanappallil P; Zimmerman AR; Cao X Enhanced lead sorption by biochar derived from anaerobically digested sugarcane bagasse. *Sep. Sci. Technol* 2011, 46 (12), 1950–1956.
- (142). Inyang M; Gao B; Yao Y; Xue Y; Zimmerman AR; Pullammanappallil P; Cao X Removal of heavy metals from aqueous solution by biochars derived from anaerobically digested biomass. *Bioresour. Technol* 2012, 110, 50–56. [PubMed: 22325901]
- (143). Lu H; Zhang W; Yang Y; Huang X; Wang S; Qiu R Relative distribution of Pb<sup>2+</sup> sorption mechanisms by sludge-derived biochar. *Water Res.* 2012, 46 (3), 854–862. [PubMed: 22189294]
- (144). Park JH; Choppala GK; Bolan N; Chung JW; Chuasavathi T Biochar reduces the bioavailability and phytotoxicity of heavy metals. *Plant Soil* 2011, 348 (1–2), 439–451.
- (145). Debela F; Thring RW; Arocena JM Immobilization of heavy metals by co-pyrolysis of contaminated soil with woody biomass. *Water, Air, Soil Pollut* 2012, 223 (3), 1161–1170.
- (146). Fang G; Gao J; Liu C; Dionysiou DD; Wang Y; Zhou D Key role of persistent free radicals in hydrogen peroxide activation by biochar: implications to organic contaminant degradation. *Environ. Sci. Technol* 2014, 48 (3), 1902–1910. [PubMed: 24422431]

- (147). Cao X; Ro KS; Chappell M; Li Y; Mao J Chemical structures of swine-manure chars produced under different carbonization conditions investigated by advanced solid-state C-13 nuclear magnetic resonance (NMR) spectroscopy. *Energy Fuels* 2011, 25, 388–397.
- (148). Uchimiya M; Orlov A; Ramakrishnan G; Sistani K In situ and ex situ spectroscopic monitoring of biochar's surface functional groups. *J. Anal. Appl. Pyrolysis* 2013, 102, 53–59.
- (149). Singh B; Fang Y; Cowie BCC; Thomsen L NEXAFS and XPS characterisation of carbon functional groups of fresh and aged biochars. *Org. Geochem.* 2014, 77, 1–10.
- (150). Cody GD; Ade H; Wirick S; Mitchell GD; Davis A Determination of chemical-structural changes in vitrinite accompanying luminescence alteration using C-NEXAFS analysis. *Org. Geochem.* 1998, 28 (7–8), 441–455.
- (151). Francis JT; Hitchcock AP Inner-shell spectroscopy of pbenzoquinone, hydroquinone, and phenol: Distinguishing quinoid and benzenoid structures. *J. Phys. Chem* 1992, 96 (16), 6598–6610.
- (152). Heymann K; Lehmann J; Solomon D; Schmidt MWI; Regier TC 1s K-edge near edge X-ray absorption fine structure (NEXAFS) spectroscopy for characterizing functional group chemistry of black carbon. *Org. Geochem* 2011, 42 (9), 1055–1064.
- (153). Schumacher M; Christ I; Scheinost AC; Jacobsen C; Kretzschmar R Chemical heterogeneity of organic soil colloids investigated by scanning transmission X-ray microscopy and C-1s NEXAFS microspectroscopy. *Environ. Sci. Technol.* 2005, 39 (23), 9094–9100. [PubMed: 16382929]
- (154). Mao JD; Johnson RL; Lehmann J; Olk DC; Neves EG; Thompson ML; Schmidt-Rohr K Abundant and stable char residues in soils: Implications for soil fertility and carbon sequestration. *Environ. Sci. Technol* 2012, 46 (17), 9571–9576. [PubMed: 22834642]
- (155). Uchimiya M; Chang S; Klasson KT Screening biochars for heavy metal retention in soil: Role of oxygen functional groups. *J. Hazard. Mater* 2011, 190 (1–3), 432–441. [PubMed: 21489689]
- (156). Dong X; Ma LQ; Zhu Y; Li Y; Gu B Mechanistic investigation of mercury sorption by Brazilian pepper biochars of different pyrolytic temperatures based on X-ray photoelectron spectroscopy and flow calorimetry. *Environ. Sci. Technol* 2013, 47 (21), 12156–12164. [PubMed: 24040905]
- (157). Uchimiya M; Bannon DI; Wartelle LH Retention of heavy metals by carboxyl functional groups of biochars in small arms range soil. *J. Agric. Food Chem* 2012, 60 (7), 1798–1809. [PubMed: 22280497]
- (158). Xu R; Zhao A; Yuan J; Jiang J pH buffering capacity of acid soils from tropical and subtropical regions of China as influenced by incorporation of crop straw biochars. *J. Soils Sediments* 2012, 12 (4), 494–502.
- (159). Jiang J; Zhang L; Wang X; Holm N; Rajagopalan K; Chen F; Ma S Highly ordered macroporous woody biochar with ultra-high carbon content as supercapacitor electrodes. *Electrochim. Acta* 2013, 113, 481–489.
- (160). Boehm HP; Heck W; Sappok R; Diehl E Surface oxides of carbon. *Angew. Chem., Int. Ed. Engl* 1964, 3 (10), 669–677.
- (161). Mukherjee A; Zimmerman AR; Harris W Surface chemistry variations among a series of laboratory-produced biochars. *Geoderma* 2011, 163 (3–4), 247–255.
- (162). Shaaban A; Se S-M; Dimin MF; Juoi JM; Husin MHM; Mitan NMM Influence of heating temperature and holding time on biochars derived from rubber wood sawdust via slow pyrolysis. *J. Anal. Appl. Pyrolysis* 2014, 107, 31–39.
- (163). Harvey OR; Herbert BE; Kuo L-J; Louchouart P Generalized two-dimensional perturbation correlation infrared spectroscopy reveals mechanisms for the development of surface charge and recalcitrance in plant-derived biochars. *Environ. Sci. Technol* 2012, 46 (19), 10641–10650. [PubMed: 22950676]
- (164). Song Y; Tahmasebi A; Yu J Co-pyrolysis of pine sawdust and lignite in a thermogravimetric analyzer and a fixed-bed reactor. *Bioresour. Technol* 2014, 174, 204–211. [PubMed: 25463801]
- (165). Uchimiya M; Wartelle LH; Klasson KT; Fortier CA; Lima IM Influence of pyrolysis temperature on biochar property and function as a heavy metal sorbent in soil. *J. Agric. Food Chem* 2011, 59 (6), 2501–2510. [PubMed: 21348519]

- (166). Teixido M; Pignatello JJ; Beltran JL; Granados M; Peccia J Speciation of the ionizable antibiotic sulfamethazine on black carbon (Biochar). *Environ. Sci. Technol* 2011, 45 (23), 10020–10027. [PubMed: 22026725]
- (167). Ni J; Pignatello JJ; Xing B Adsorption of aromatic carboxylate ions to black carbon (biochar) is accompanied by proton exchange with water. *Environ. Sci. Technol* 2011, 45 (21), 9240–9248. [PubMed: 21999243]
- (168.) Yang G; Jiang H Amino modification of biochar for enhanced adsorption of copper ions from synthetic wastewater. *Water Res.* 2014, 48, 396–405. [PubMed: 24183556]
- (169). Qian L; Chen M; Chen B Competitive adsorption of cadmium and aluminum onto fresh and oxidized biochars during aging processes. *J. Soils Sediments* 2015, 15 (5), 1130–1138.
- (170). Abit SM; Bolster CH; Cai P; Walker SL Influence of feedstock and pyrolysis temperature of biochar amendments on transport of *Escherichia coli* in saturated and unsaturated soil. *Environ. Sci. Technol* 2012, 46 (15), 8097–8105. [PubMed: 22738035]
- (171). Fang Q; Chen B; Lin Y; Guan Y Aromatic and hydrophobic surfaces of wood-derived biochar enhance perchlorate adsorption via hydrogen bonding to oxygen-containing organic groups. *Environ. Sci. Technol* 2014, 48 (1), 279–288. [PubMed: 24289306]
- (172). Wang D; Zhang W; Hao X; Zhou D Transport of biochar particles in saturated granular media: effects of pyrolysis temperature and particle size. *Environ. Sci. Technol* 2013, 47 (2), 821–828. [PubMed: 23249307]
- (173). Liao S; Pan B; Li H; Zhang D; Xing B Detecting free radicals in biochars and determining their ability to inhibit the germination and growth of corn, wheat and rice seedlings. *Environ. Sci. Technol* 2014, 48 (15), 8581–8587. [PubMed: 24988274]
- (174). Bohm H; Jander H; Tanke D PAH growth and soot formation in the pyrolysis of acetylene and benzene at high temperatures and pressures: Modeling and experiment. *Symp. (Int.) Combust., [Proc.]* 1998, 27, 1605–1612.
- (175). Qiu N; Li H; Jin Z; Zhu Y Temperature and time effect on the concentrations of free radicals in coal: Evidence from laboratory pyrolysis experiments. *Int. J. Coal Geol* 2007, 69 (3), 220–228.
- (176). Fang G; Liu C; Gao J; Dionysiou DD; Zhou D Manipulation of persistent free radicals in biochar to activate persulfate for contaminant degradation. *Environ. Sci. Technol* 2015, 49 (9), 5645–5653. [PubMed: 25864382]
- (177). Fang G; Zhu C; Dionysiou DD; Gao J; Zhou D Mechanism of hydroxyl radical generation from biochar suspensions: Implications to diethyl phthalate degradation. *Bioresour. Technol* 2015, 176, 210–217. [PubMed: 25461005]
- (178). Kluepfel L; Keiluweit M; Kleber M; Sander M Redox properties of plant biomass-derived black carbon (biochar). *Environ. Sci. Technol* 2014, 48 (10), 5601–5611. [PubMed: 24749810]
- (179). Buss W; Masek O Mobile organic compounds in biochar - A potential source of contamination - Phytotoxic effects on cress seed (*Lepidium sativum*) germination. *J. Environ. Manage* 2014, 137, 111–119. [PubMed: 24608115]
- (180). Oleszczuk P; Josko I; Kusmierz M Biochar properties regarding to contaminants content and ecotoxicological assessment. *J. Hazard. Mater* 2013, 260, 375–382. [PubMed: 23792930]
- (181). Spokas KA; Novak JM; Stewart CE; Cantrell KB; Uchimiya M; DuSaire MG; Ro KS Qualitative analysis of volatile organic compounds on biochar. *Chemosphere* 2011, 85 (5), 869–882. [PubMed: 21788060]
- (182). Kaal J; Martinez Cortizas A; Reyes O; Solino M Molecular characterization of *Ulex europaeus* biochar obtained from laboratory heat treatment experiments - A pyrolysis-GC/MS study. *J. Anal. Appl. Pyrolysis* 2012, 95, 205–212.
- (183). Becker R; Dorgerloh U; Helmig M; Mumme J; Diakite M; Nehls I Hydrothermally carbonized plant materials: Patterns of volatile organic compounds detected by gas chromatography. *Bioresour. Technol* 2013, 130, 621–628. [PubMed: 23334019]
- (184). Freddo A; Cai C; Reid BJ Environmental contextualisation of potential toxic elements and polycyclic aromatic hydrocarbons in biochar. *Environ. Pollut* 2012, 171, 18–24. [PubMed: 22863991]
- (185). Hale SE; Lehmann J; Rutherford D; Zimmerman AR; Bachmann RT; Shitumbanuma V; O'Toole A; Sundqvist KL; Arp HPH; Cornelissen G Quantifying the total and bioavailable

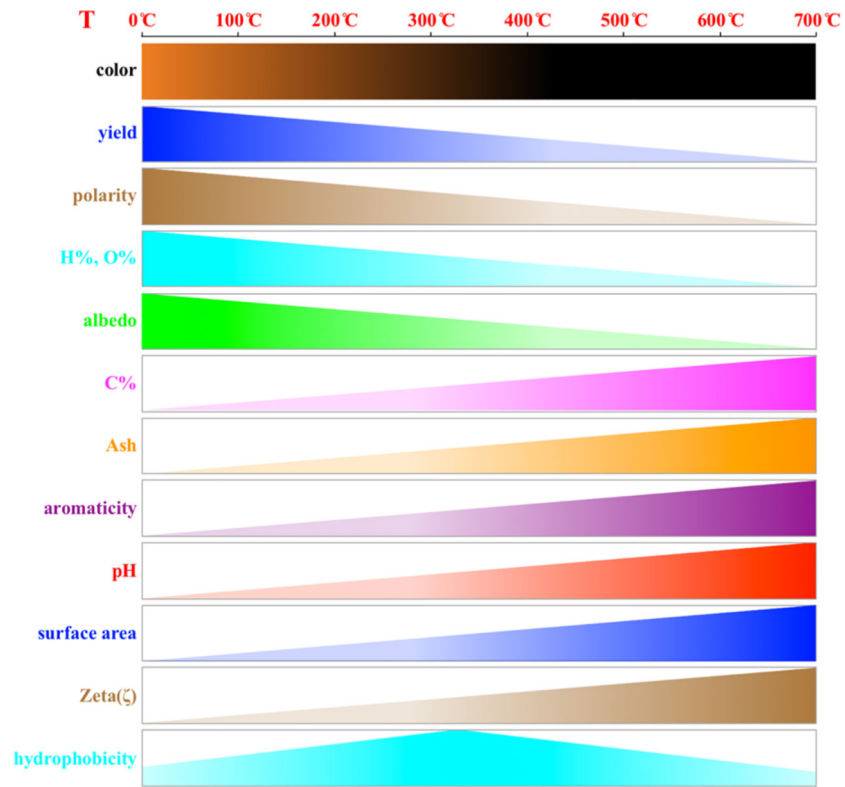
- polycyclic aromatic hydrocarbons and dioxins in biochars. *Environ. Sci. Technol* 2012, 46 (5), 2830–2838. [PubMed: 22321025]
- (186). Hilber I; Blum F; Leifeld J; Schmidt H-P; Bucheli TD Quantitative determination of PAHs in biochar: A prerequisite to ensure its quality and safe application. *J. Agric. Food Chem* 2012, 60 (12), 3042–3050. [PubMed: 22397545]
- (187). Keiluweit M; Kleber M; Sparrow MA; Simoneit BRT; Prahlg FG Solvent-extractable polycyclic aromatic hydrocarbons in biochar: Influence of pyrolysis temperature and feedstock. *Environ. Sci. Technol* 2012, 46 (17), 9333–9341. [PubMed: 22844988]
- (188). Koltowski M; Oleszczuk P Toxicity of biochars after polycyclic aromatic hydrocarbons removal by thermal treatment. *Ecol. Eng* 2015, 75, 79–85.
- (189). Quilliam RS; Rangelcroft S; Emmett BA; DeLuca TH; Jones DL Is biochar a source or sink for polycyclic aromatic hydrocarbon (PAH) compounds in agricultural soils? *GCB Bioenergy* 2013, 5 (2), 96–103.
- (190). Zielinska A; Oleszczuk P The conversion of sewage sludge into biochar reduces polycyclic aromatic hydrocarbon content and ecotoxicity but increases trace metal content. *Biomass Bioenergy* 2015, 75, 235–244.
- (191). Kloss S; Zehetner F; Dellantonio A; Hamid R; Ottner F; Liedtke V; Schwanninger M; Gerzabek MH; Soja G Characterization of slow pyrolysis biochars: Effects of feedstocks and pyrolysis temperature on biochar properties. *J. Environ. Qual* 2012, 41 (4), 990–1000. [PubMed: 22751041]
- (192). Oleszczuk P; Zielinska A; Cornelissen G Stabilization of sewage sludge by different biochars towards reducing freely dissolved polycyclic aromatic hydrocarbons (PAHs) content. *Bioresour. Technol* 2014, 156, 139–145. [PubMed: 24495539]
- (193). Becker L; Bada JL; Winans RE; Hunt JE; Bunch TE; French BM Fullerenes in the 1.85-billion-year-old sudbury impact structure. *Science* 1994, 265 (5172), 642–645. [PubMed: 11536660]
- (194). Crombie K; Masek O; Sohi SP; Brownsort P; Cross A The effect of pyrolysis conditions on biochar stability as determined by three methods. *GCB Bioenergy* 2013, 5 (2), 122–131.
- (195). Spokas KA; Novak JM; Masiello CA; Johnson MG; Colosky EC; Ippolito JA; Trigo C Physical disintegration of biochar: An overlooked process. *Environ. Sci. Technol. Lett* 2014, 1 (8), 326–332.
- (196). Chen D; Yu X; Song C; Pang X; Huang J; Li Y Effect of pyrolysis temperature on the chemical oxidation stability of bamboo biochar. *Bioresour. Technol* 2016, 218, 1303–1306. [PubMed: 27481469]
- (197). Fang Y; Singh B; Singh BP Effect of temperature on biochar priming effects and its stability in soils. *Soil Biol. Biochem* 2015, 80, 136–145.
- (198). Harvey OR; Kuo L-J; Zimmerman AR; Louchouart P; Amonette JE; Herbert BE An index-based approach to assessing recalcitrance and soil carbon sequestration potential of engineered black carbons (Biochars). *Environ. Sci. Technol* 2012, 46 (3), 1415–1421. [PubMed: 22242866]
- (199). Kim S; Kramer RW; Hatcher PG Graphical method for analysis of ultrahigh-resolution broadband mass spectra of natural organic matter, the van Krevelen diagram. *Anal. Chem* 2003, 75 (20), 5336–5344. [PubMed: 14710810]
- (200). Lehmann J; Joseph S *Biochar for Environmental Management: Science, Technology and Implementation*; Taylor & Francis: Boca Raton, FL, 2015.
- (201). Naisse C; Girardin C; Lefevre R; Pozzi A; Maas R; Stark A; Rumpel C Effect of physical weathering on the carbon sequestration potential of biochars and hydrochars in soil. *GCB Bioenergy* 2015, 7 (3), 488–496.
- (202). Zimmermann M; Bird MI; Wurster C; Saiz G; Goodrick I; Barta J; Capek P; Santruckova H; Smernik R Rapid degradation of pyrogenic carbon. *Global Change Biol.* 2012, 18 (11), 3306–3316.
- (203). Naisse C; Alexis M; Plante A; Wiedner K; Glaser B; Pozzi A; Carcaillet C; Criscuoli I; Rumpel C Can biochar and hydrochar stability be assessed with chemical methods? *Org. Geochem.* 2013, 60, 40–44.
- (204). Creamer AE; Gao B; Zhang M Carbon dioxide capture using biochar produced from sugarcane bagasse and hickory wood. *Chem. Eng. J* 2014, 249, 174–179.

- (205). Bolan NS; Kunhikrishnan A; Choppala GK; Thangarajan R; Chung JW Stabilization of carbon in composts and biochars in relation to carbon sequestration and soil fertility. *Sci. Total Environ.* 2012, 424, 264–270. [PubMed: 22444054]
- (206). Qayyum MF; Steffens D; Reisenauer HP; Schubert S Kinetics of carbon mineralization of biochars compared with wheat straw in three soils. *J. Environ. Qual* 2012, 41 (4), 1210–1220. [PubMed: 22751064]
- (207). Hua L; Zhang C; Ma H; Yu W Environmental benefits of biochar made by agricultural straw when applied to soil. *Ecol. Environ. Sci* 2010, 19 (10), 2489–2492.
- (208). Schulz H; Dunst G; Glaser B Positive effects of composted biochar on plant growth and soil fertility. *Agron. Sustainable Dev* 2013, 33 (4), 817–827.
- (209). Liu J; Schulz H; Brandl S; Miehtke H; Huwe B; Glaser B Short-term effect of biochar and compost on soil fertility and water status of a Dystric Cambisol in NE Germany under field conditions. *J. Plant Nutr. Soil Sci* 2012, 175 (5), 698–707.
- (210). Jones DL; Rousk J; Edwards-Jones G; DeLuca TH; Murphy DV Biochar-mediated changes in soil quality and plant growth in a three year field trial. *Soil Biol. Biochem* 2012, 45, 113–124.
- (211.) Wardle DA; Nilsson M-C; Zackrisson O Fire-derived charcoal causes loss of forest humus. *Science* 2008, 320 (5876), 629–629. [PubMed: 18451294]
- (212). Luo Y; Durenkamp M; De Nobili M; Lin Q; Brookes PC Short term soil priming effects and the mineralisation of biochar following its incorporation to soils of different pH. *Soil Biol. Biochem* 2011, 43 (11), 2304–2314.
- (213). Kuzyakov Y; Subbotina I; Chen H; Bogomolova I; Xu X Black carbon decomposition and incorporation into soil microbial biomass estimated by C-14 labeling. *Soil Biol. Biochem* 2009, 41 (2), 210–219.
- (214). Lu W; Ding W; Zhang J; Li Y; Luo J; Bolan N; Xie Z Biochar suppressed the decomposition of organic carbon in a cultivated sandy loam soil: A negative priming effect. *Soil Biol. Biochem* 2014, 76, 12–21.
- (215). Santos F; Torn MS; Bird JA Biological degradation of pyrogenic organic matter in temperate forest soils. *Soil Biol. Biochem* 2012, 51, 115–124.
- (216). Abiven S; Andreoli R Charcoal does not change the decomposition rate of mixed litters in a mineral cambisol: a controlled conditions study. *Biol. Fertil. Soils* 2011, 47 (1), 111–114.
- (217). Maestrini B; Nannipieri P; Abiven S A meta-analysis on pyrogenic organic matter induced priming effect. *GCB Bioenergy* 2015, 7 (4), 577–590.
- (218). Zimmerman AR; Gao B; Ahn M-Y Positive and negative carbon mineralization priming effects among a variety of biochar-amended soils. *Soil Biol. Biochem* 2011, 43 (6), 1169–1179.
- (219). Bell MJ; Worrall F Charcoal addition to soils in NE England: A carbon sink with environmental co-benefits? *Sci. Total Environ* 2011, 409 (9), 1704–1714. [PubMed: 21329965]
- (220). Singh BP; Cowie AL Long-term influence of biochar on native organic carbon mineralisation in a low-carbon clayey soil. *Sci. Rep* 2015, 4, No. 3687.
- (221). Kuang C; Jiang C; Li Z; Hu F Effects of biochar amendments on soil organic carbon mineralization and microbial biomass in red paddy soils. *Soils* 2012, 44 (4), 570–575.
- (222). Ronsse F; van Hecke S; Dickinson D; Prins W Production and characterization of slow pyrolysis biochar: influence of feedstock type and pyrolysis conditions. *GCB Bioenergy* 2013, 5 (2), 104–115.
- (223). Steinbeiss S; Gleixner G; Antonietti M Effect of biochar amendment on soil carbon balance and soil microbial activity. *Soil Biol. Biochem* 2009, 41 (6), 1301–1310.
- (224). Dempster DN; Gleeson DB; Solaiman ZM; Jones DL; Murphy DV Decreased soil microbial biomass and nitrogen mineralisation with Eucalyptus biochar addition to a coarse textured soil. *Plant Soil* 2012, 354 (1–2), 311–324.
- (225). Zhao Z; Zhang Y; Woodard TL; Nevin KP; Lovley DR Enhancing syntrophic metabolism in up-flow anaerobic sludge blanket reactors with conductive carbon materials. *Bioresour. Technol* 2015, 191, 140–145. [PubMed: 25989089]
- (226). Chen S; Rotaru A-E; Shrestha PM; Malvankar NS; Liu F; Fan W; Nevin KP; Lovley DR Promoting interspecies electron transfer with biochar. *Sci. Rep* 2015, 4, No. 5019.

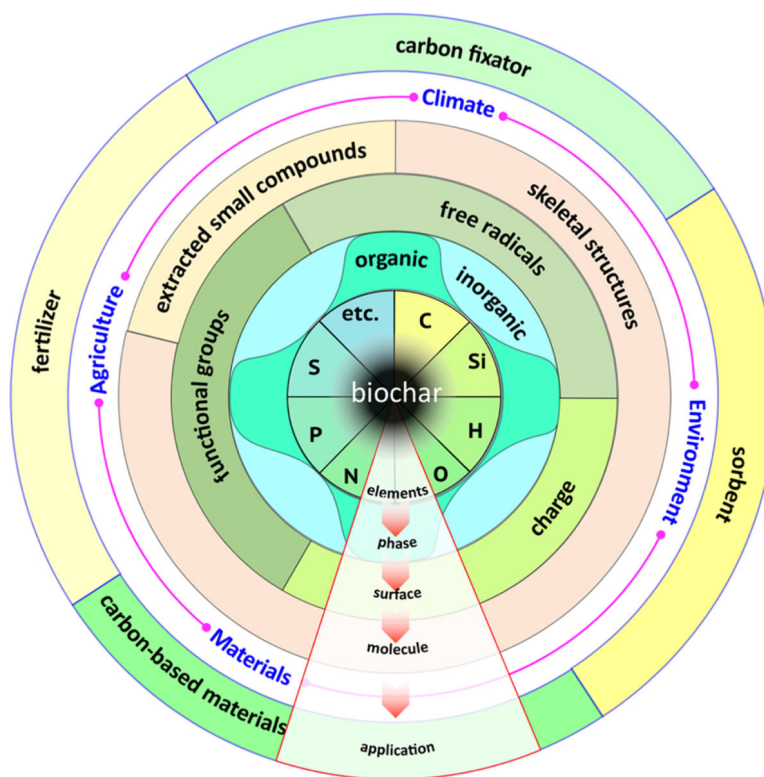


- (227). Kappler A; Wuestner ML; Ruecker A; Harter J; Halama M; Behrens S Biochar as an electron shuttle between bacteria and Fe(III) minerals. *Environ. Sci. Technol. Lett* 2014, 1 (8), 339–344.
- (228). Chen B; Yuan M; Qian L Enhanced bioremediation of PAH-contaminated soil by immobilized bacteria with plant residue and biochar as carriers. *J. Soils Sediments* 2012, 12 (9), 1350–1359.
- (229.) Renner R Rethinking biochar. *Environ. Sci. Technol.* 2007, 41 (17), 5932–5933. [PubMed: 17937262]
- (230). Wang J; Zhang M; Xiong Z; Liu P; Pan G Effects of biochar addition on N<sub>2</sub>O and CO<sub>2</sub> emissions from two paddy soils. *Biol. Fertil. Soils* 2011, 47 (8), 887–896.
- (231). Wang J; Pan X; Liu Y; Zhang X; Xiong Z Effects of biochar amendment in two soils on greenhouse gas emissions and crop production. *Plant Soil* 2012, 360 (1–2), 287–298.
- (232). Dong D; Yang M; Wang C; Wang H; Li Y; Luo J; Wu W Responses of methane emissions and rice yield to applications of biochar and straw in a paddy field. *J. Soils Sediments* 2013, 13 (8), 1450–1460.
- (233.) Sarkhot DV; Berhe AA; Ghezzehei TA Impact of biochar enriched with dairy manure effluent on carbon and nitrogen dynamics. *J. Environ. Qual* 2012, 41 (4), 1107–1114. [PubMed: 22751052]
- (234). Liu Y; Yang M; Wu Y; Wang H; Chen Y; Wu W Reducing CH<sub>4</sub> and CO<sub>2</sub> emissions from waterlogged paddy soil with biochar. *J. Soils Sediments* 2011, 11 (6), 930–939.
- (235). Scheer C; Grace PR; Rowlings DW; Kimber S; Van Zwieten L Effect of biochar amendment on the soil-atmosphere exchange of greenhouse gases from an intensive subtropical pasture in northern New South Wales, Australia. *Plant Soil* 2011, 345 (1–2), 47–58.
- (236). Troy SM; Lawlor PG; O' Flynn CJ; Healy MG Impact of biochar addition to soil on greenhouse gas emissions following pig manure application. *Soil Biol. Biochem* 2013, 60, 173–181.
- (237). Spokas KA Impact of biochar field aging on laboratory greenhouse gas production potentials. *GCB Bioenergy* 2013, 5 (2), 165–176.
- (238). Feng Y; Xu Y; Yu Y; Xie Z; Lin X Mechanisms of biochar decreasing methane emission from Chinese paddy soils. *Soil Biol. Biochem* 2012, 46, 80–88.
- (239). Peters JF; Iribarren D; Dufour J Biomass pyrolysis for biochar or energy applications? A life cycle assessment. *Environ. Sci. Technol* 2015, 49 (8), 5195–5202. [PubMed: 25830564]
- (240). Ibarrola R; Shackley S; Hammond J Pyrolysis biochar systems for recovering biodegradable materials: A life cycle carbon assessment. *Waste Manage.* 2012, 32 (5), 859–868.
- (241). Roberts KG; Gloy BA; Joseph S; Scott NR; Lehmann J Life cycle assessment of biochar systems: Estimating the energetic, economic, and climate change potential. *Environ. Sci. Technol* 2010, 44 (2), 827–833. [PubMed: 20030368]
- (242). Conley DJ; Paerl HW; Howarth RW; Boesch DF; Seitzinger SP; Havens KE; Lancelot C; Likens GE Ecology controlling eutrophication: Nitrogen and phosphorus. *Science* 2009, 323 (5917), 1014–1015. [PubMed: 19229022]
- (243). Zheng H; Wang Z; Deng X; Zhao J; Luo Y; Novak J; Herbert S; Xing B Characteristics and nutrient values of biochars produced from giant reed at different temperatures. *Bioresour. Technol* 2013, 130, 463–471. [PubMed: 23313694]
- (244). Liu P; Ptacek CJ; Blowes DW; Landis RC Mechanisms of mercury removal by biochars produced from different feedstocks determined using X-ray absorption spectroscopy. *J. Hazard. Mater* 2016, 308, 233–242. [PubMed: 26844404]
- (245). Chen Z; Chen B; Chiou CT Fast and slow rates of naphthalene sorption to biochars produced at different temperatures. *Environ. Sci. Technol* 2012, 46 (20), 11104–11111. [PubMed: 22970831]
- (246). Chen Z; Chen B; Zhou D; Chen W Bisolute sorption and thermodynamic behavior of organic pollutants to biomass-derived biochars at two pyrolytic temperatures. *Environ. Sci. Technol* 2012, 46 (22), 12476–12483. [PubMed: 23121559]
- (247). Zhang W; Sun H; Wang L Influence of the interactions between black carbon and soil constituents on the sorption of pyrene. *Soil Sediment Contam.* 2013, 22 (4), 469–482.
- (248). Zhang M; Gao B; Varmoosfaderani S; Hebard A; Yao Y; Inyang M Preparation and characterization of a novel magnetic biochar for arsenic removal. *Bioresour. Technol* 2013, 130, 457–462. [PubMed: 23313693]

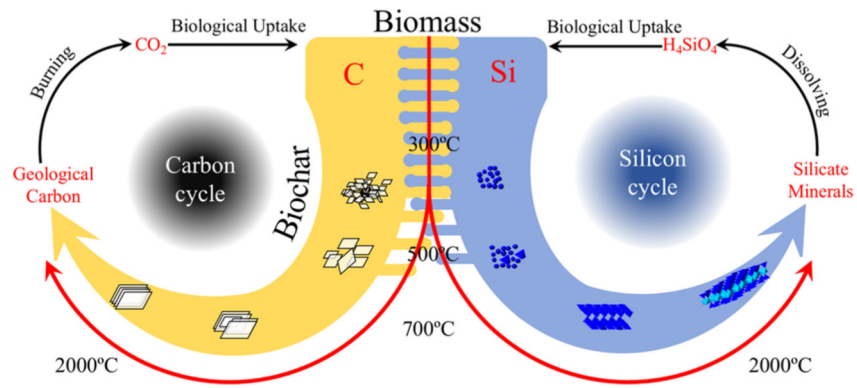
- (249). Ippolito JA; Strawn DG; Scheckel KG; Novak JM; Ahmedna M; Niandou MAS Macroscopic and molecular investigations of copper sorption by a steam-activated biochar. *J. Environ. Qual* 2012, 41 (4), 1150–1156. [PubMed: 22751057]
- (250). Zhang F; Wang X; Yin D; Peng B; Tan C; Liu Y; Tan X; Wu S Efficiency and mechanisms of Cd removal from aqueous solution by biochar derived from water hyacinth (*Eichornia crassipes*). *J. Environ. Manage* 2015, 153, 68–73. [PubMed: 25660498]
- (251). Xu R; Xiao S; Yuan J; Zhao A Adsorption of methyl violet from aqueous solutions by the biochars derived from crop residues. *Bioresour. Technol* 2011, 102 (22), 10293–10298. [PubMed: 21924897]
- (252). Yang Y; Lin X; Wei B; Zhao Y; Wang J Evaluation of adsorption potential of bamboo biochar for metal-complex dye: equilibrium, kinetics and artificial neural network modeling. *Int. J. Environ. Sci. Technol* 2014, 11 (4), 1093–1100.
- (253). Essandoh M; Kunwar B; Pittman CU, Jr.; Mohan D; Mlsna T Sorptive removal of salicylic acid and ibuprofen from aqueous solutions using pine wood fast pyrolysis biochar. *Chem. Eng. J* 2015, 265, 219–227.
- (254). Xie M; Chen W; Xu Z; Zheng S; Zhu D Adsorption of sulfonamides to demineralized pine wood biochars prepared under different thermochemical conditions. *Environ. Pollut* 2014, 186, 187–194. [PubMed: 24384578]
- (255). Chen Z; Fang Y; Xu Y; Chen B Adsorption of Pb<sup>2+</sup> by rice straw derived-biochar and its influential factors. *Acta Scientiae Circumstantiae* 2012, 32 (4), 769–776.
- (256). An Z; Hou Y; Cai C; Xue X Lead(II) adsorption characteristics on different biochars derived from rice straw. *Environ. Chem* 2011, 30 (11), 1851–1857.
- (257). Liu J; Chen X; Wang Y; Strathmann TJ; Werth CJ Mechanism and mitigation of the decomposition of an oxorhenium complex-based heterogeneous catalyst for perchlorate reduction in water. *Environ. Sci. Technol* 2015, 49 (21), 12932–12940. [PubMed: 26422179]
- (258). Huggins T; Wang HM; Kearns J; Jenkins P; Ren ZJ Biochar as a sustainable electrode material for electricity production in microbial fuel cells. *Bioresour. Technol* 2014, 157, 114–119. [PubMed: 24534792]
- (259). Lobo FL; Wang H; Huggins T; Rosenblum J; Linden KG; Ren ZJ Low-energy hydraulic fracturing wastewater treatment via AC powered electrocoagulation with biochar. *J. Hazard. Mater* 2016, 309, 180–184. [PubMed: 26894291]



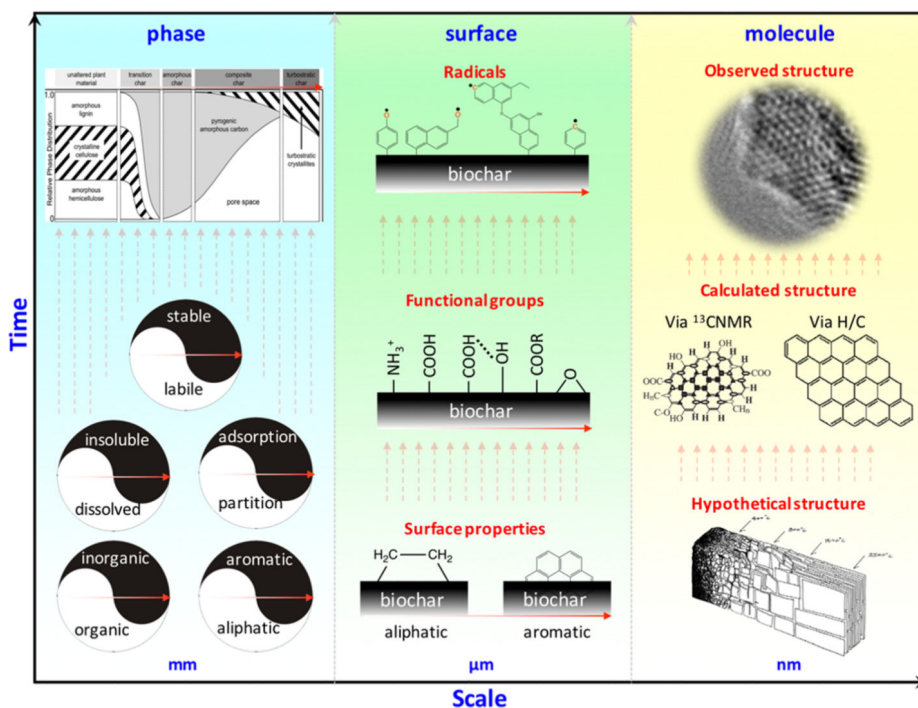
**Figure 1.** Biochar property variations with increased pyrolysis temperatures.



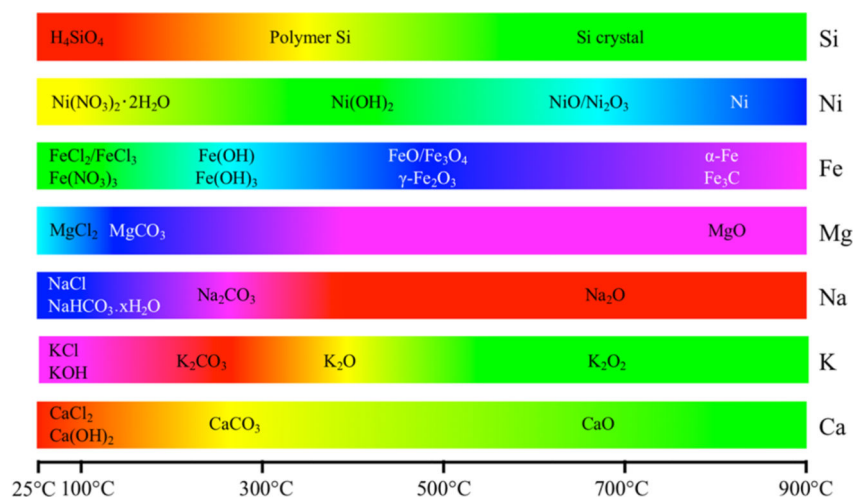
**Figure 2.** Heterogeneous structures and potential applications of biochar from a consideration of the elemental composition, phase, surface chemistry, and molecular structure.



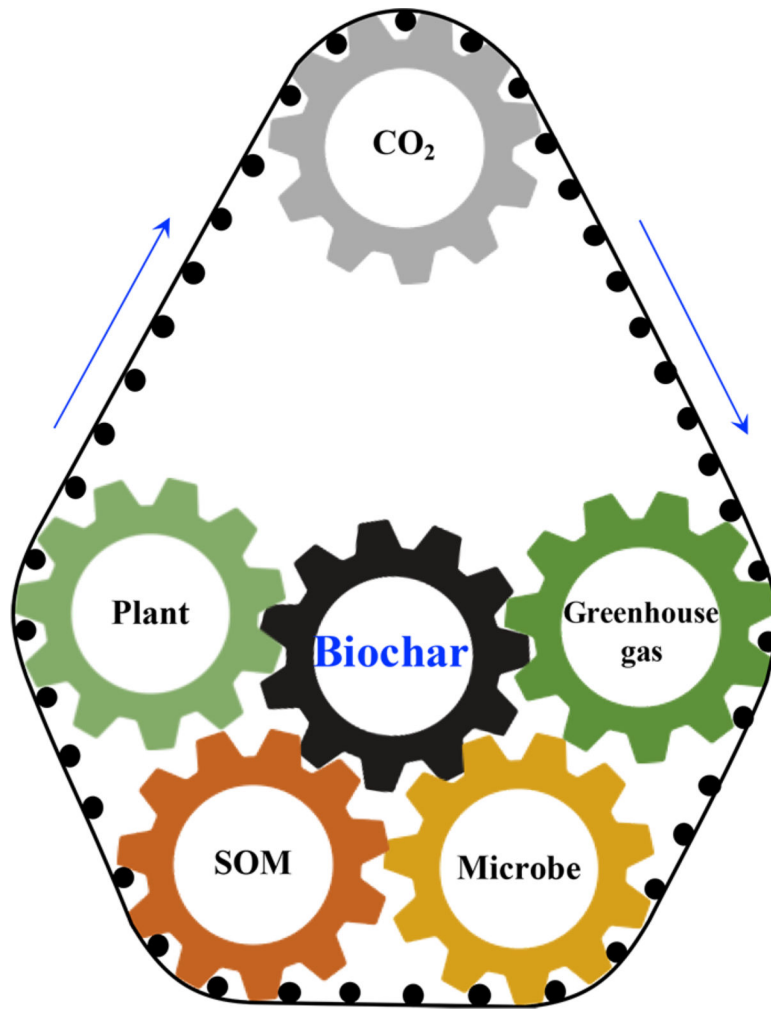
**Figure 3.** Carbon and silicon cycles along with the carbon–silicon coupling relationship in biochar and the terrestrial ecosystem.



**Figure 4.** Knowledge evolution concerning the phases, surface chemistry, and molecular structure of biochars as a function of the inverse biochar scale (size) and research time. Inner figures were cited from refs 1, 21, 22, 40, 119. Copyright 2010, 2016, 2017 American Chemical Society.

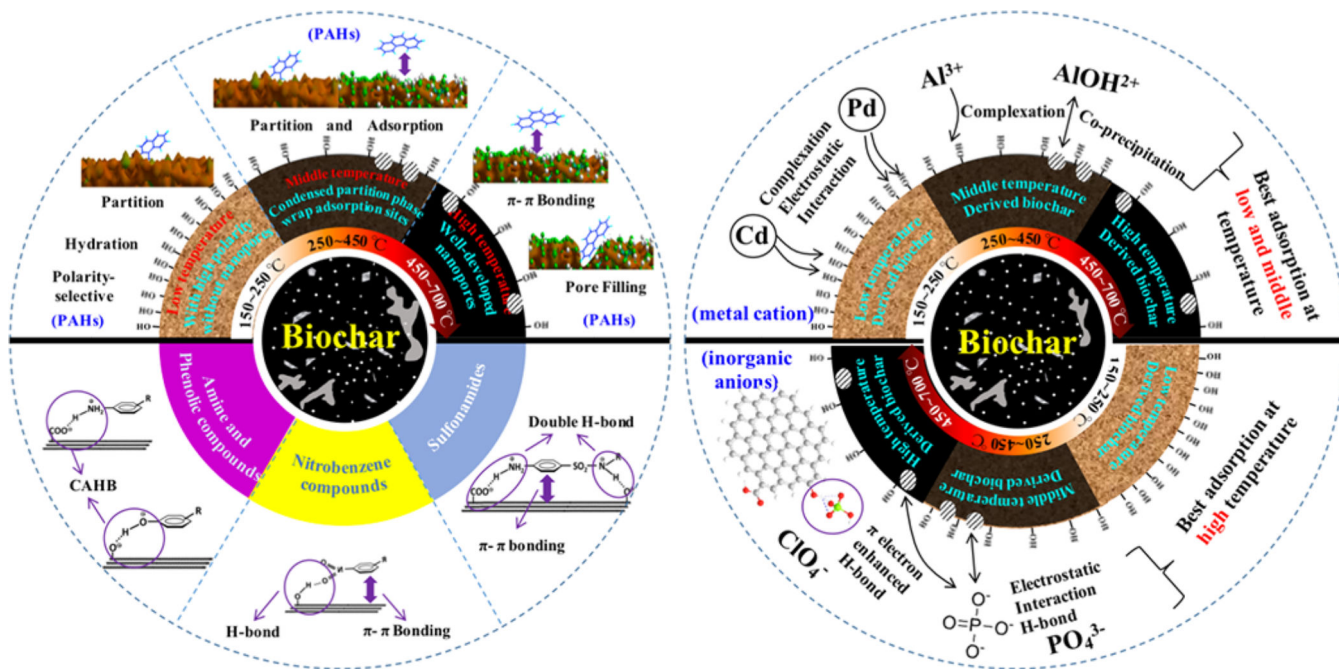


**Figure 5.** Possible phase and chemical transformations of several mineral components during biomass pyrolysis under limited oxygen. For each inorganic element, the color illustrates the corresponding transition from one state to another. Cited from the corresponding references: Si,<sup>14</sup> Ni,<sup>37</sup> Fe,<sup>37,122,123</sup> and Mg.<sup>34,35</sup>



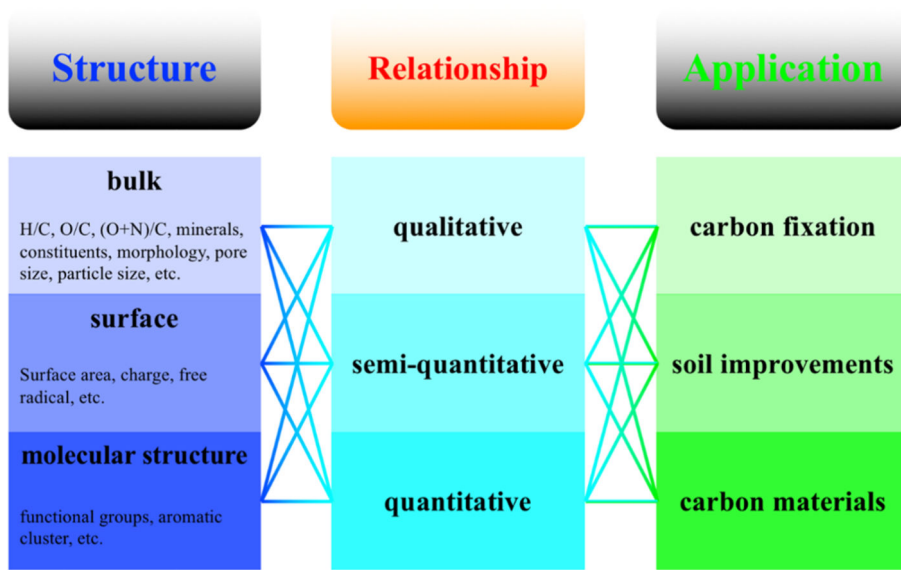
**Figure 6.** Factors affecting biochar stability as well as net carbon sequestration and, in turn, positive biochar effects on plant vegetation and soil properties.





**Figure 7.**


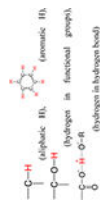
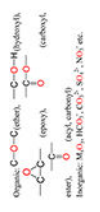
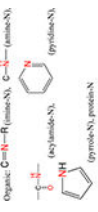
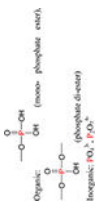

Sorption mechanisms of organic (left) and inorganic pollutants (right) to biochars prepared under different pyrolytic temperatures. PAHs: polycyclic aromatic hydrocarbons. CAHB: charge-assisted H-bond, including negative charge-assisted H-bond (–) CAHB and positive charge-assisted H-bond (+) CAHB.



**Figure 8.** Structure–application relationships of biochars.

**Table 1.**

**Species, Functions, and Applications of Selected Elements within Biochars**

Elements	Species	Functions
C	 <p>Organic: C-C (single bond), C=C (double bond), C-X (functionalized carbon) Inorganic: H<sub>2</sub>O, CO<sub>2</sub></p>	<p>a) Key element within biochars;                      b) Develop functional groups by linking to other elements;                      c) Inorganic carbon contributes to the alkalinity and buffering properties of biochars;<sup>23</sup>                      d) Carbon sequestration.<sup>9</sup></p>
Si	Inorganic: Silicon acid, polymeric Si, crystal Si.	<p>a) Nutrient element;                      b) Co-precipitator with heavy metals,<sup>24</sup>                      c) Major element of biochar inorganic phases;<sup>14</sup>                      d) Protect the organic phase.<sup>14</sup></p>
H	 <p>Aliphatic H, Aromatic H, Hydrogen in functional groups, Hydrogen in hydrogen bond</p>	<p>a) For association/ dissociation;                      b) To form the hydrogen bond;<sup>25</sup>                      c) H/C atomic ratio is the aromaticity index of biochars.<sup>22</sup></p>
O	 <p>Organic: C-O-C (ether), C-O-H (hydroxyl), (epoxy), (oxyl, carbonyl) ester, Inorganic: MO<sub>2</sub>, HCO<sub>3</sub><sup>-</sup>, CO<sub>3</sub><sup>2-</sup>, SO<sub>4</sub><sup>2-</sup>, NO<sub>3</sub><sup>-</sup> etc.</p>	<p>a) To form the functional groups;                      b) Complexation with metal ions;<sup>26</sup>                      c) O/C atomic ratio is an index of the degree of aging of biochars.<sup>27</sup></p>
N	 <p>Organic: C-N-R (amine), C=N (nitrile), (pyrimidin-N), (pyridin-N), (pyrrolidin-N) Inorganic: NH<sub>3</sub>, NH<sub>4</sub><sup>+</sup>, NO<sub>2</sub><sup>-</sup>, NO<sub>3</sub><sup>-</sup></p>	<p>a) Nutrient element;                      b) Improve the thermal stability;                      c) Active sites for reaction and modification;                      d) Nitrogen fixation.<sup>28</sup></p>
P	 <p>Organic: (mono- phosphate ester), (phosphate di-ester) Inorganic: PO<sub>4</sub><sup>3-</sup>, P<sub>2</sub>O<sub>5</sub></p>	<p>a) Nutrient element;                      b) Precipitator with heavy metals.<sup>11</sup></p>
S	 <p>Organic: (sulfonamide) Inorganic: sulfide</p>	<p>a) Increase the solubility of carbon materials;<sup>29</sup>                      b) Solid acid catalyst;<sup>30</sup>                      c) Nutrient element.</p>

Elements	Species	Functions
Fe	Fe <sub>2</sub> O <sub>3</sub> , Fe <sub>3</sub> O <sub>4</sub> , FeO, α-Fe, Fe <sub>3</sub> C, FeO(OH), Zero valent iron, other metal complex	<ul style="list-style-type: none"> <li>a) Provide magnetism;<sup>31</sup></li> <li>b) Increase the sorption ability for anions;<sup>31</sup></li> <li>c) Promote graphitizing during pyrolysis;<sup>32</sup></li> <li>d) Catalysis/activator for organic pollutant degradation.<sup>33</sup></li> </ul>
Mg	MgO, MgCO <sub>3</sub> , other metal complex	<ul style="list-style-type: none"> <li>a) Increase anions sorption;<sup>34</sup></li> <li>b) CO<sub>2</sub> capture;<sup>35</sup></li> <li>c) Nutrient element.</li> </ul>
Mn	MnO <sub>x</sub> , Mn(OH) <sub>x</sub> , other metal complex	<ul style="list-style-type: none"> <li>a) Increase heavy metal sorption;<sup>36</sup></li> <li>b) Increase capacity.</li> </ul>
Ni	Ni(OH) <sub>2</sub> , NiO, Ni <sub>2</sub> O <sub>3</sub> , other metal complex	<ul style="list-style-type: none"> <li>a) H<sub>2</sub> evolution;</li> <li>b) Catalysis the formation of syngas during pyrolysis.<sup>37</sup></li> </ul>